

See discussions, stats, and author profiles for this publication at: <https://www.researchgate.net/publication/26835049>

Total Synthesis and Biological Evaluation of (+)- and (-)-Bisanthraquinone Antibiotic BE-43472B and Related Compounds

ARTICLE *in* JOURNAL OF THE AMERICAN CHEMICAL SOCIETY · SEPTEMBER 2009

Impact Factor: 12.11 · DOI: 10.1021/ja9073694 · Source: PubMed

CITATIONS

20

READS

28

6 AUTHORS, INCLUDING:



Jochen Becker

Evonik Industries

16 PUBLICATIONS 159 CITATIONS

[SEE PROFILE](#)



Ana Montero

The Scripps Research Institute

29 PUBLICATIONS 628 CITATIONS

[SEE PROFILE](#)



NIH Public Access

Author Manuscript

J Am Chem Soc. Author manuscript; available in PMC 2010 October 21.

Published in final edited form as:

J Am Chem Soc. 2009 October 21; 131(41): 14812–14826. doi:10.1021/ja9073694.

Total Synthesis and Biological Evaluation of (+)- and (-)-Bisanthraquinone Antibiotic BE-43472B and Related Compounds

K. C. Nicolaou, Jochen Becker, Yee Hwee Lim, Alexandre Lemire, Thomas Neubauer, and Ana Montero

Department of Chemistry and The Skaggs Institute for Chemical Biology, The Scripps Research Institute, 10550 North Torrey Pines Road, La Jolla, California 92037, and the Department of Chemistry and Biochemistry, University of California, San Diego, 9500 Gilman Drive, La Jolla, California 92093

Abstract

The bisanthraquinone antibiotic BE-43472B [(+)-**1**] was isolated by Rowley and coworkers from a streptomycete strain found in a green algae associated with the ascidian *Ecteinascidia turbinata* and has shown promising antibacterial activity against clinically derived isolates of methicillin-susceptible, methicillin-resistant, and tetracyclin-resistant *Staphylococcus aureus* (MSSA, MRSA, and TRSA, respectively), and vancomycin-resistant *Enterococcus faecalis* (VRE). Described herein is the first total synthesis of both enantiomers of this bisanthraquinone antibiotic, the determination of its absolute configuration, as well as the biological evaluation of these and related compounds. The developed synthesis relies on a highly efficient cascade sequence involving an intermolecular Diels–Alder reaction between diene (*R*)-**61** and dienophile **55** followed by an intramolecular nucleophilic aromatic *ipso* substitution. Late stage transformations included a remarkable photochemical α,β -epoxyketone rearrangement [**80** \rightarrow (+)-**1**]. Interestingly, the unnatural enantiomer [(-)-**1**] of antibiotic BE-43472B exhibited comparable antibacterial properties to those of the natural enantiomer [(+)-**1**].

Introduction

Bisanthraquinones **1** and **3** (Figure 1) were reported by Rowley and co-workers as two naturally occurring antibiotics with biological activities against drug resistant bacteria.^{1,2} Possessing striking molecular architectures, these compounds were isolated by these researchers from *Streptomyces* strain #N1-78-1 which was isolated from cultured cells of an unidentified unicellular green algae (URI strain #N36-11-10) extracted from the ascidian *Ecteinascidia turbinata*, collected from La Parguera, Puerto Rico. Interestingly, the gross structures of these compounds, and their mono-methylated siblings **2** and **4** (Figure 1), were previously reported in a Japanese patent as anti-tumor agents.³ Isolated from *Streptomyces* sp. A43472, these compounds were designated in this patent as BE-43472A (**3**), BE-43472B (**1**), BE-43472C (**4**) and BE-43472D (**2**). Although the Rowley group was able to assign the complete relative stereochemistry of the bisanthraquinone antibiotics BE-43472B (**1**) and BE-43472A (**3**) on the basis of NMR spectroscopic analysis, and to point out their likely identities to those isolated by the Japanese workers, they left their absolute configuration unassigned.^{1,2}

kcn@scripps.edu.

Supporting Information Available: Experimental procedures and full compound characterization. This material is available free of charge via the Internet at <http://pubs.acs.org>.

These bisanthraquinone antibiotics exhibited, in addition to anti-tumor properties, impressive inhibitory activities against a variety of bacteria.^{1,2} Antibiotic BE-43472B (**1**) demonstrated potent inhibitory activities against an expanded panel of clinical bacterial isolates of Gram-positive pathogens, including methicillin-susceptible *Staphylococcus aureus* [MSSA, MIC₅₀ = 0.11 μM (range 0.054–0.22, 25 isolates)], methicillin-resistant *Staphylococcus aureus* [MRSA, MIC₅₀ = 0.23 μM (range 0.11–0.90, 25 isolates)], vancomycin-resistant *Enterococcus faecalis* [VRE, MIC₅₀ = 0.90 μM (range 0.22–3.6), 25 isolates] and tetracycline-resistant *Staphylococcus aureus* [TRSA, MIC₅₀ = 0.11 μM (range 0.11–0.23, 11 isolates)]. Most significantly, in a time-kill study, BE-43472B (**1**) exhibited strong bactericidal activity (>99.9% kill) against MSSA, MRSA and VRE.² This compound was found to possess no activity against the Gram-negative pathogens *Klebsiella pneumoniae* (ATCC 700603) and *Escherichia coli* (ATCC 35218) while it demonstrated significant potency (IC₅₀ = 2.0 μM) against the human colon cancer cell line HCT-116.

In view of the continuing search for new antibacterial agents to combat infections due to drug-resistant bacteria,⁴ and because of the unprecedented structures of these new antibiotics, their chemical synthesis was deemed important.⁵ In a recent communication, we reported the first total synthesis and absolute configuration of bisanthraquinone antibiotic BE-43472B (**1**) and its enantiomer (Figure 2).^{6,7} In this article, we provide the full account of our work in this area that includes the evolution of the synthetic strategy toward both enantiomers of **1** and the construction of a number of analogues of this unusual antibiotic.

Results and Discussion

General Retrosynthetic Analysis. The Michael Reaction Approach

The T-shaped molecular architecture of the bisanthraquinone antibiotics as exemplified by BE-43472B (**1**) is both unprecedented and challenging from the synthetic point of view. Its C₃₂H₂₄O₉ formula reveals its highly conjugated/unsaturated nature with two non-identical anthraquinone moieties serving as its two dominant regions. These domains are fused together through a bicyclic system comprised of two 5-membered rings, each containing an oxygen atom and featuring a ketal functionality. The two anthraquinone structural motifs are held together by a crowded carbon–carbon bond and a carbon–oxygen–carbon bridge. Its five stereogenic centers reside in a cluster resulting in considerable distortion of the molecule's otherwise flat regions. Figure 2 presents the two enantiomeric forms of BE-43472B (**1**) and their computer energy-minimized frame models. Since the absolute stereochemistry of the target molecule was unknown at the outset of our work, our synthetic plan had to accommodate both enantiomers, one at a time, from readily available starting materials and with subsequent stereocontrol.

In our initial retrosynthetic analysis, shown in Scheme 1 (with the originally depicted^{1,2} absolute configuration, which eventually turned out to be the antipodal to that of the natural product), we first removed the rather labile C-3 hydroxyl group¹ and protected the two phenolic groups of the BE-43472B (**1**) molecule to reveal structure **5** as a potential precursor to our target. By removing the C-3 hydroxyl group, we ensured stability for the intermediates on the way toward the final stages where we would seek an opportunity to install it. The ketal functionality within the advanced precursor **5** was then dismantled, unraveling intermediate **6**, protected at the secondary alcohol site. Holding the two, now conspicuous anthraquinone moieties together in **6** was only a single bond (C-4a–C-7'). This key carbon–carbon bond was envisioned to be formed through a Michael-type addition of the enolate derived from bromoketone **8** (or its debromo analogue) to enetriione **7**, followed by HBr elimination and aromatization (or oxidation/aromatization) to generate the requisite phenolic structural motif of **6** (R = H or protecting group in **5**–**7**).

Initial Model Studies. Formation of Key Carbon–Carbon Bond and Aromatization

In order to test the feasibility of the key carbon–carbon bond (C-4a–C-7') forming step of our designed strategy toward antibiotic BE-43472B (**1**), a model study was undertaken using simplified aryl ketone **9** as the donor and quinone **10** as the acceptor in the projected Michael reaction (Scheme 2). Thus, exposure of the known aryl ketone **9⁸** to LiHMDS (1.0 equiv, THF, -78 °C) followed by quenching of the resulting enolate with enetrione **10^{8,9}** furnished, in quantitative yield, the desired racemic Michael adducts **11** and *epi*-**11**, which upon flash column chromatography (silica) equilibrated to ca. 1:1 mixture of inseparable epimers. Fortunately, crystallization from acetone led to preferential formation of crystals of **11** (m.p. = 188–190 °C, acetone), whose structure was proven by X-ray crystallographic analysis (see ORTEP drawing, Figure 3). This crystallographic analysis not only proved the identity of the two epimers, but also confirmed the regiochemical outcome of the addition of the enolate of **9** to the enetrione system (**10**).

Having achieved the requisite carbon–carbon bond formation, we then turned our attention to the oxidation/aromatization of the so-obtained product (**11**). However, the seemingly simple task of aromatizing ring F of this product proved much more challenging than expected. Thus, and much to our dismay, all attempts (e.g. exposure to acids, bases, heat, microwave conditions) at aromatizing and/or oxidizing ring F of adduct **11** proved in vain, leading only to decomposition (mainly retro-Michael products) or non-selective oxidations to an array of unidentified products. In the end, a way forward was found by abandoning ketone **9** and resorting to bromoketone **12** as a “pre-oxidized” substrate for the Michael reaction with enetrione **10** (Scheme 2). Thus, treatment of bromoketone **12** (prepared from **9** by exposure to NBS) with LiHMDS (1.0 equiv, THF, -78 °C), followed by reaction of the generated enolate with enetrione **10** (1.1 equiv), resulted in the formation of Michael adduct **13**, albeit in lower yield than before (63%). It was interesting, however, to observe in this case that only a single diastereomer (stereochemistry unassigned) of **13** was observed (by ¹H NMR spectroscopy). Exposure of this adduct to CAN in MeCN:H₂O (2:1) at 0 °C led to concurrent oxidation of the protected hydroquinone ring G, HBr elimination, and aromatization of ring F to furnish the desired phenolic quinone **14** in a pleasing 93% yield. It was with these encouraging results that we embarked on our first attempt to synthesize BE-43472B (**1**) using the Michael reaction as the key step to unite the two bisanthraquinone fragments of the molecule.

Initial Approach Toward BE-43472B. Synthesis of Building Blocks

Having completed successfully the model study for the projected Michael addition/aromatization approach to antibiotic BE-43472B (**1**), we then proceeded to construct the required building blocks for the natural product, quinone **7** and bromoketone **8** (Scheme 1). For building block **8** and related fragments, we developed an improved synthesis through modification of our previous route⁸ based on the Hauser annulation reaction. The required nitrile components **19a** and **19b** were prepared as shown in Scheme 3. Thus, exposure of 4-methylsalicylic acid (**15**) to oxalyl chloride (1.2 equiv) in the presence of catalytic amounts of DMF in CH₂Cl₂ followed by reaction of the resulting acid chloride with either Et₂NH•HCl (1.3 equiv), or Me₂NH•HCl (1.3 equiv) afforded phenolic amides **16a** (74% yield) or **16b** (88% yield), respectively. These intermediates (**16a** or **16b**) served as precursors to the corresponding protected derivatives (**17a** or **17b**) which were prepared by protection of the free phenolic hydroxy group either with a PMB (PMBCl, K₂CO₃, *n*-Bu₄NI cat., 99% yield of **17a**), or a MOM (MOMCl, *i*-Pr₂NET, 97% yield of **17b**) group. *o*-Lithiation¹⁰ of aryl amides **17a** or **17b** (*t*-BuLi, THF, -78 °C) followed by quenching with freshly distilled DMF furnished aldehydes **18a** or **18b** in 67 and 95% yield, respectively. Treatment of aldehydes **18a** or **18b** with TMSCN in the presence of catalytic amounts of KCN and 18-crown-6, followed by quenching with AcOH, then led to nitriles **19a** or **19b** in 76 and 85% yield, respectively, as shown in Scheme 3.

The conversions of nitriles **19a** and **19b** to the desired bromoketone **8**, hydroquinone derivatives **21–23** and bromoanthracene **26** (which were also called upon to act as Michael-donors later on in the campaign, *vide infra*) through a Hauser annulation¹¹ are shown in Scheme 4. Thus, treatment of **19a** or **19b** with LiHMDS in THF at –78 °C followed by addition of cyclohex-2-enone (**20**) gave the corresponding dihydroquinones, which upon methylation (Cs_2CO_3 , Me_2SO_4) led to methylated ketones **21a** (37% yield from aldehyde **18a** over the three steps) or **21b** (59% yield from nitrile **19a** over the two steps), respectively. Treatment of ketone **21a** with 1.0 equiv of LiHMDS in THF at –78 °C, followed by quenching with 1.0 equiv of NBS, furnished the desired bromoketone **8** in 51% yield. On the other hand, the use of 2.4 equiv of LiHMDS and 2.0 equiv of NBS in the above reaction led to dibromoketone **24**, which upon exposure to DBU furnished bromoanthracene **25**, demonstrating that the aromatization of such systems is possible, and providing access to aryl bromide precursors for coupling reactions with suitable Michael acceptors. Finally, protection of the phenolic group within **25** with MOMCl (Cs_2CO_3) led to MOM derivative **26** in 28% overall yield for the three steps.

The required quinone fragment **7a** and related compounds **7b** and **7c** were envisaged to be constructed through a route featuring a diastereoselective Diels–Alder reaction between chiral diene **33a** and juglone (**35**) as the dienophile.¹² The requisite diene **33a** was synthesized starting from (S)-ethyl lactate and 2-butyn-1-ol (**27**) as outlined in Scheme 5.¹³ Thus, addition of Red-Al to alkynol **27** in ether at –78 → 25 °C,¹⁴ followed by quenching the resulting aluminate with iodine furnished, upon protection with MEMCl, vinyl iodide MEM ether **29** in 88% overall yield. A Nozaki–Hiyama–Kishi coupling¹⁵ of **29** with known lactaldehyde (S)-(-)-**30a**¹⁶ mediated by $\text{CrCl}_2\text{-NiCl}_2$ afforded a mixture of *syn* and *anti* alcohols **31a** and **31b** (ca. 4:1 ratio) in 90% yield. Reaction of this mixture (or each of the chromatographically separated diastereomers) with MOMCl and *i*-Pr₂NEt led to the corresponding MOM derivatives (**32a** and **32b**, 91 and 90% yield, respectively), which underwent 1,4-elimination on exposure to *s*-BuLi in THF at –78 °C to afford diene **33a**, in 76% yield.¹⁷ Finally, removal of the TBDPs group from the latter compound with TBAF gave hydroxy diene **34** in 94% yield, as shown in Scheme 5.

As depicted in Scheme 6, reaction of diene **33a** with juglone (**35**, 1.3 equiv) proceeded smoothly in CH_2Cl_2 (ambient temperature, 48 h) to afford Diels–Alder adduct **38** as the major product, together with its regioisomer **39** (81% combined yield, ca. 5:1 ratio). These compounds proved to be rather labile due to their susceptibility toward oxidation by atmospheric oxygen and partial decomposition on silica gel through elimination of the OMEM group. Stereoselective hydrogenation (10% Pd/C, MeOH) of the crude Diels–Alder reaction mixture gave the more stable adducts **40** and **41** in 59 and 15% yield starting from **33a**, respectively. While the regioselectivity of this Diels–Alder reaction was expected on the basis of electronic complementarity [dominating FMO interactions between the dienophile (C-2, δ^+) and the diene (C-4, δ^-), see structures **35** and **33a**, Scheme 6], its facial selectivity required consideration of steric factors in order to trace its origins. Thus, minimization of 1,3-allylic strain within the conformation of diene **33a** and minimization of steric repulsion in the transition states TS-**36** and TS-**37** may explain the exquisite diastereoselectivity in the formation of both regioisomers **38** and **39**.

Proceeding with the synthesis, exposure of the major regioisomer **40** to MnO_2 in CH_2Cl_2 at ambient temperature furnished the desired quinone **42a** in 88% yield (Scheme 7). Treatment of the latter compound with ZnBr_2 (CH_2Cl_2 , 25 °C) furnished, in quantitative yield, hydroxy compound **43a**, whose oxidation to the targeted quinone **7a** was accomplished with IBX (MeCN, 50 °C, 94% yield). Alternatively, phenolic quinone **42a** was first protected, either as benzyl ether (BnBr , Ag_2O , DMF, in the dark) to afford **42b** (86% yield), or *p*-nitrobenzyl ether (*p*-NO₂BnBr, Ag_2O , DMF, in the dark), to furnish **42c** (quantitative yield). Exposure of the latter compounds to aqueous HCl in MeOH led to the corresponding alcohols (**43b** or **43c**),

which were subsequently oxidized with IBX (MeCN, 50 °C) to afford quinone **7b** (89% yield) or **7c** (78% yield), respectively. *p*-Nitrobenzyl quinone derivative **7c** crystallized in beautiful yellow-orange crystals (m.p. = 159–161 °C, H₂O/MeCN) whose X-ray crystallographic analysis (see ORTEP drawing, Figure 5) proved its absolute configuration and confirmed the initial structural assignment of the Diels–Alder adduct **38** (Scheme 6).

Coupling of the Two Fragments Through Michael-Type Reaction and Further Exploration Toward the Target Molecule

With the two key requisite building blocks for the construction of the target molecule now available, we set out to explore their coupling through the intended Michael addition/aromatization sequence along the pathway to antibiotic BE-43472B (**1**). Scheme 8 summarizes our advances and setbacks as we attempted to break through certain barriers toward the target molecule. Initial reaction of the enolate of **21a** with Michael acceptor anthraquinone **7a** (R = H, see Scheme 7) had shown to result in low conversion, presumably due to protonation of the enolate by the free phenol moiety of **7a**. Thus, treatment of aryl ketone **21a** with LiHMDS (1.0 equiv) in THF at –78 °C, followed by addition of benzyl-protected quinone **7b** (–78 → 25 °C), furnished adduct **44a** in 31% yield as a mixture of diastereomers (ca. 1:1), isomerizing over time to a single diastereomer (stereochemistry unassigned).

Unfortunately, exposure of bromoketone **8** (see Scheme 4) to the same conditions as those shown in Scheme 8 failed to produce any coupling product, presumably due to the steric bulk of the bromine residue. This hypothesis prompted us to synthesize the corresponding fluoroketone **22** (X = F, Scheme 8) by quenching the enolate of ketone **21a** (LiHMDS) with (PhSO₂)NF (98% yield, see Scheme 4) in order to explore its coupling with Michael acceptor **7b**. In the event, the enolate of **22** reacted with enetriione **7b** to afford the desired product (**44b**), albeit in only 11% yield, as a mixture of diastereomers (ca. 1:1 ratio) as shown in Scheme 8. A number of other partners, including *p*-nitrobenzyl quinone **7c** and regiosomeric bromoketone **23** (prepared from ketone **21b** by heating at 70 °C with NBS in the presence of AIBN in benzene, 52% yield, see Scheme 4), were also explored for their reactivity toward the desired goal. Thus, partnering fluoroketone **22** with quinone **7c** under the developed coupling conditions led to a very low yield (9%) of adduct **44c** (ca. 1:1 mixture of diastereomers), while the union of the regiosomeric bromoketone **23** with quinone **7b** under the standard conditions led to **45** in 49% yield (ca. 1:1 mixture of diastereoisomers), as shown in Scheme 8. However, aromatization attempts to convert these adducts to the desired anthraquinone systems **6** (Scheme 1) proved in vain, as only decomposition and undesired products, primarily due to retro-Michael reactions, were observed. In order to avoid the problem of the competing retro-Michael reactions, the coupling of the aromatized bromoanthracene **26** (see Scheme 4) and enetriione **7b** via metalation and various cross-coupling type reactions was investigated. Disappointingly, all attempts to form the challenging C-7'-C-4a bond failed. Faced with low yields in the Michael coupling reactions and the inability to form the desired anthraquinone **6** from the resulting products, we decided to abort this approach and seek, instead, an entirely new strategy for the set goal of synthesizing BE-43472B (**1**).

Second Generation Diels–Alder Approach. The All-Carbon Skeleton Encompassing Strategy

Despite our failure to reach the desired framework of the BE-43472B molecule (**1**) through the Michael reaction/aromatization approach, during these studies we came to recognize the usefulness of the Diels–Alder reaction in forming the C-ring of our target. In a speculative, but daring move we considered generating the entire carbon skeleton of the antibiotic **1** through a Diels–Alder reaction-based strategy between the appropriate components. This second generation Diels–Alder approach is shown retrosynthetically in Scheme 9 using the structure depicted by (–)-**1** (although at this stage we did not know the absolute stereochemistry of the natural product as mentioned above). Thus, dehydrating (–)-**1** retrosynthetically toward the

enol moiety led to conjugated system **46**, whose forward manipulation would require regio- and stereoselective epoxidation, followed by regioselective opening of the resulting oxirane, to afford the natural product. Dismantling of the two 5-membered ether rings within the latter intermediate through sequential C–O bond disconnections, insertion of a MeO group at C-8', and reduction of the enol moiety revealed structure **47** as a possible precursor to **46**. Applying a retro Diels–Alder reaction on **47** unraveled diene **34** and dienophile **48** as the required building blocks for this strategy. The adoption of diene **34** was based on our findings regarding its regiochemical reactivity toward juglone (**35**) as discussed above (Scheme 6), which was expected to favor the desired regiosomeric Diels–Alder product. This expectation was in part based on wishful thinking, since at this stage we were cognizant of the uncertainty surrounding the regio- and stereochemical outcome of the designed Diels–Alder reaction because we were unsure about the overall electronic effect of the anthraquinone moiety attached onto the juglone structural motif within dienophile **48**. The answer would come through experimentation as we shall describe below.

The construction of dienophile **48** commenced from hydroanthracene **21b** (see Scheme 4 for preparation) and proceeded as summarized in Scheme 10. Thus, treatment of **21b** with LiHMDS in the presence of NBS produced dibromoketone **49** in 98% yield, whose aromatization (DBU) and methylation (Cs_2CO_3 , Me_2SO_4) furnished aryl bromide **51** (74% overall yield over two steps) through intermediate phenol **50**. Oxidation of **51** with CAN afforded anthraquinone **52** (77% yield), which reacted with $\text{Me}_3\text{SnSnMe}_3$ in the presence of $\text{Pd}(\text{PPh}_3)_4$ catalyst to afford trimethyl stannane **53** in 94% yield. Stille coupling^{18,19} of **53** with bromoquinone **54**²⁰ proceeded smoothly in the presence of catalytic amounts of $\text{Pd}(\text{PPh}_3)_4$ and CuI, furnishing the desired dienophile **48** in 65% yield. Later on, the MOM group was removed from the latter compound (1% HCl in MeOH, 85% yield) to generate the diphenolic compound **55**, which was subsequently also called upon to act as a dienophile in these studies.

Scheme 11 presents the results of the Diels–Alder reaction between diene **34** and dienophile **48**. Thus, heating a mixture of **34** (4.0 equiv) with **48** (1.0 equiv) in benzene at 80 °C for 72 h furnished a single Diels–Alder adduct whose structure was determined, through subsequent chemistry and NMR spectroscopy, to be that of the undesired regioisomer **57**.^{21,22} Interestingly, the silylated dienes **33a** and **33b** (prepared through a similar route as that shown in Scheme 5 for **33a**) failed to react with dienophile quinone **48** under various conditions, presumably due to steric hindrance, underscoring the relevance of the free secondary alcohol in the diene system to the success of the Diels–Alder reaction. Exposure of adduct **57** to the action of ZnBr_2 resulted in the simultaneous removal of the MOM and MEM protecting groups and the formation of the isomeric heptacyclic lactols **58a** and **58b** (84% yield, ca. 1:1 ratio, not separable by chromatography). Their structures were determined through ^1H NMR ROESY studies that revealed the NOEs indicated on their structures in Scheme 11. Manual molecular models are supportive of the rotational barrier between these two atropisomeric structures (**58a** and **58b**). These studies also provided the crucial evidence for the regioisomeric nature of the Diels–Alder adduct **57**, apparently formed through *endo* transition state TS–**56** which is favored over its regioisomeric transition state TS–**56'** that was expected to form the desired adduct **47** as shown in Scheme 11. The stereochemistry of compounds **57** and **58a/58b** could not be completely discerned through NMR spectroscopy. It was presumed to be as shown on the basis of the most favorable facial orientation of diene **34** and dienophile **48** as they merge through transition state TS–**56** (Scheme 11) to form the Diels–Alder product **57**. However, from these failed experiments we draw the conclusion that the electronic (–I) effect of the electron withdrawing anthraquinone substituent attached onto the juglone dienophile overrides the polarizing effect of the intramolecular H-bond within this system,²³ enlarging the C-3 orbital coefficient of the LUMO of the juglone system. The overall polarized characters of diene **34** and dienophile **48** (as shown in **34'** and **48'**, Scheme 11) dictate the regiochemical outcome of

their union to afford cycloadduct **57**. This path-pointing study led us to the next phase of our campaign toward the total synthesis of antibiotic BE-43472B (**1**).

Final Diels–Alder Approach. Total Synthesis of Antibiotic BE-43472B

Based on the latest intelligence gathering, we redesigned our second generation Diels–Alder strategy toward the target molecule in order to accommodate the realities of the electronics within the dienophile component of the cycloaddition reaction. Scheme 12 outlines, in retrosynthetic format, the newly devised synthetic strategy. Note that in this Scheme we again use the antipodal structure [(-)-**1**] of the natural product (we will switch to the structure of the enantiomer (+)-**1** in our final drive toward BE-43472B). The main provision in this plan was the adoption of diene (*S*)-**61** (with a 2-oxa as opposed to a 1-oxa substituent), which was expected to possess the reverse polarity (enlargement of the C-1 orbital coefficient of the HOMO) from that of the originally used diene (**34**), and therefore match the demonstrated polarity of dienophile **55** (see Scheme 12). The adoption of (*S*)-**61**, in turn, required placement of an oxygen atom at C-2 within the Diels–Alder product (*ent*-**60**) that would have to be subsequently removed. Additionally, two new oxygen atoms will have to be introduced into the emerging structures (*ent*-**60** and *ent*-**59**) at C-3 and C-1 before reaching (−)-**1**. Another interesting feature of the new synthetic design was the choice of the naked dienophile **55**, whose anthraquinone intramolecular H-bonding was expected to facilitate the intended intramolecular *ipso* substitution in order to cast the last bond of the ring framework of the target molecule. These new design modifications highlighted our expectations for success with the possibility of a cascade sequence, beginning with the Diels–Alder reaction and ending with an octacyclic structure, whose molecular complexity would be impressively close to that of the targeted natural product.

The required diene (*S*)-**61** became readily available through the concise synthetic route summarized in Scheme 13. Reaction of commercially available phosphorane **62** with known aldehyde (S)-(−)-**30b**²⁴ gave α,β -unsaturated ester (*S*)-**63** in 92% yield (E:Z > 98:2), which was first converted to Weinreb amide (*S*)-**64** through the action of HNMe(OMe) and Me₂AlCl and then to methyl ketone (*S*)-**65** by reaction with MeLi (77% yield for the two steps).²⁵ Desilylation of the latter compound with TBAF led to hydroxy ketone (*S*)-**66** (93% yield), which was treated with 2.3 equiv of LDA, to afford, after quenching the resulting dianion with 1.0 equiv TBSOTf, diene (*S*)-**61** in 33% yield and 95% *ee*, as determined by HPLC analysis using a chiral column (plus 47% recovered starting material).

At this stage, and in order to obtain insight into the behavior of (*S*)-**61** toward relevant quinone-type dienophiles, this diene was allowed to react with juglone (**35**). As shown in Scheme 14, the reaction proceeded in CH₂Cl₂ at room temperature, leading, as expected, to the opposite regioisomer (i.e. **68**, >9:1 regioselectivity) to that obtained previously with the terminally (1-oxa) substituted diene (**33a**, see Scheme 6). However, in this case the resulting Diels–Alder product (**68**) was found to be rather labile, undergoing facile oxidation by air in the presence of silica gel, forming quinone **69** (62% yield overall from **35**). The regiochemical identity of **69** was based on HMBC NMR correlations as designated in Scheme 14, while the stereochemistry of its precursor (**68**) was based on transition state TS-**67** as the sterically most favorable (1,3-allylic strain). This regio- and stereochemical outcome pointed to the high likelihood that diene (*S*)-**61** will react with dienophile **55** with the desired regio- and diastereoselectivity.

Indeed, the Diels–Alder reaction between diene (*S*)-**61** and dienophile **55** this time proceeded as planned, and was followed by a pleasing sequence of transformations that eventually led to a successful total synthesis (vide infra). However, the obtained synthetic BE-43472B exhibited the opposite optical rotation to that exhibited by the natural BE-43472B, an observation that led to the true configurational identity of the natural product. Thus, by utilizing diene (*S*)-**61**

we reached the enantiomer of BE-43472B [(-)-**1**, Figure 2]. We then synthesized diene (*R*)-**61** starting with aldehyde (*R*)-(+) -**30b** and entered it into the developed synthetic sequence, arriving at BE-43472B in its naturally occurring enantiomeric form [(+)-**1**, Figure 2]. It is this sequence that we now describe below.

Scheme 15 depicts the first phase of the reaction sequence that was initiated upon mixing (*R*)-**61** and dienophile **55**. Thus, heating (*R*)-**61** (2.0 equiv) with **55** (1.0 equiv) in CH_2Cl_2 solution in a sealed tube (85 °C external temperature) for 48 h, followed by addition of toluene and refluxing with a Dean–Stark apparatus for another 24 h, led, through a remarkable cascade sequence,²⁶ to an inconsequential mixture of the two C-9a epimers **72** and 9a-*epi*-**72** (9a-*epi*-**72:****72** ca. 2:1) in a 98% combined yield. This aesthetically pleasing cascade became possible only because the initial Diels–Alder cycloaddition reaction proceeded, through transition state **TS-70**, regio- and stereoselectively, as desired. The resulting cycloadduct **60** was observed by NMR spectroscopic analysis to exist in equilibrium with its hemiketal form **59** (**59:****60** ca. 4:1, benzene-*d*₆). Inspection of manual molecular models indicates that hemiketal **59** finds itself poised and in a favorable conformation to undergo an intramolecular aromatic *ipso* substitution [$\text{S}_{\text{N}}(\text{Ar})$ -type intramolecular transesterification], expelling a molecule of MeOH to form octacycle **72** through tetrahedral intermediate **71** as shown in Scheme 15. The presence of the adjacent β-phenolic quinone moiety apparently facilitates this novel cyclization through internal H-bonding, which activates the vinylogous-type ester for the initiating attack by the hemiketal hydroxyl group as shown in structures **59** and **71**. Under the toluene azeotropic refluxing conditions that removed the released MeOH from the reaction mixture, product **72** suffers epimerization at C-9a to afford 9a-*epi*-**72**, a phenomenon also observed on silica gel. In refluxing benzene, we also observed (by ¹H NMR spectroscopy) epimerization of **59** to 9a-*epi*-**59** as shown in Scheme 15. With ample amounts of **72** and 9a-*epi*-**72** in hand, the stage was now set for an attempt to reach the final target, antibiotic BE-43472B [(+)-**1**].

The obligatory employment of diene (*R*)-**61** in our synthesis necessitated excision of the superfluous oxygen atom from the C-2 position of the growing molecule; furthermore, two new oxygen atoms, one at C-1 and one at C-3, had to be introduced in their proper positions before the final target could be reached. These objectives were achieved as shown in Scheme 16. Thus, treatment of the mixture of 9a-*epi*-**72** and **72** (ca. 2:1 ratio)²⁷ with *m*-CPBA at –20 °C led to a mixture of four oxirane epimers (ca. 4:1 ratio of β:α oxirane pairs, α-epimers not shown). Desilylation of these oxiranes as a mixture (HF•py, TMSOMe) was accompanied by ring opening to afford a mixture of four hydroxy ketones (**74**, ca. 4:1 β:α ratio, α-epimers not shown), which were subsequently, and without isolation, subjected to SeO_2 oxidation in AcOH (120 °C) to afford enone **75** (49% overall for the three steps) together with its C-3 epimer (3-*epi*-**75**, 39%, chromatographically separated), indicating that epimerization of the C-3 stereogenic center took place under the oxidation conditions. Crystallization of **75** from CH_2Cl_2 led to single crystals (m.p. >250 °C, CH_2Cl_2 /hexanes), whose X-ray crystallographic analysis (see ORTEP drawing, Figure 5) revealed its relative configuration and confirmed the stereochemical outcomes of both the Diels–Alder and the epoxidation reactions. Having accomplished the installation of the C-3 hydroxyl group in its desired configuration, we then proceeded to address the challenging task of selectively removing the superfluous oxygen atom from C-2. To this end, and as shown in Scheme 16, we subjected enone **75** to the action of ethane-1,2-dithiol under various conditions. After considerable experimentation we found that reaction of the enantiomeric ketone *ent*-**75** with 4.0 equiv ethane-1,2-dithiol and 6.0 equiv $\text{BF}_3\bullet\text{OEt}_2$ in CH_2Cl_2 led to dithioketal *ent*-**76** (55% yield), in which the C-9 carbonyl group (activated through intramolecular H-bonding) was preferentially protected out of the four carbonyl moieties present in the substrate (i.e. *ent*-**75**). Using ethane-1,2-dithiol as solvent and 2.6 equiv of $\text{BF}_3\bullet\text{OEt}_2$ improved the efficiency of this reaction, furnishing *ent*-**76** in 78% yield. However, when the reaction was carried out with enone **75** under more forcing conditions (ethane-1,2-dithiol as solvent, 15 equiv $\text{BF}_3\bullet\text{OEt}_2$), followed by quenching with 0.1 M HCl,

the desired C-2 dithioketal **78** was isolated in 63% yield, presumably through intermediate bis-dithioketal **77**, which apparently collapses upon exposure to H₂O by hydrolysis of the C-9 dithiolane. The latter process is rendered facile and selective, presumably through intramolecular H-bonding of the phenolic OH with the neighboring sulfur atom, now made possible by the increased electron density on the latter as a result of the suppression of the electron withdrawing effect of the C-2 carbonyl moiety (upon its engagement as a dithiolane system). This remarkably selective reaction offered the sought-after window of opportunity for the desired C-2 deoxygenation, which was accomplished through reductive desulfurization (Raney-Ni 2400) to afford compound **79** in 45% yield (plus 19% recovered starting material; 56% yield brsm). With this operation behind us, all that remained to reach the target molecule was the insertion of an oxygen atom in the C–H bond of the enone moiety within **79**.

Having failed to achieve a direct Wacker-type oxidation²⁸ of enone **79**, and due to the ease of elimination of the axial C-3 hydroxyl group of the natural product [(+)-**1**],¹ we resorted to the mild two-step procedure involving epoxidation/oxirane rearrangement²⁹ as shown in Scheme 17. Thus, epoxidation of **79** with *t*-BuOOH and DBU furnished the β-oxirane **80** as the major product (84% yield), together with small amounts of the epimeric α-oxirane (*α*-**80**, 7% yield, chromatographically separated). While a number of metal- and Lewis acid-catalyzed protocols failed to induce the desired transformation of epoxy ketone **80** to the natural product, simple irradiation of this precursor in benzene with UV light at ambient temperature (and in the absence of any sensitizer) smoothly converted it to bisantraquinone antibiotic BE-43472B [(+)-**1**] in 77% yield (83% yield based on 92% conversion). Synthetic (+)-**1** exhibited identical physical properties to those reported for the natural product and essentially the same optical rotation $[\alpha]_D^{20}$ (*c* = 0.14 in CHCl₃) = +411.4 as that of natural (+)-**1** $[\alpha]_D^{20}$ (*c* = 0.14 in CHCl₃) = +403.1, and so did (−)-**1**, except for its optical rotation, which was of the opposite sign $[\alpha]_D^{20}$ (*c* = 0.14 in CHCl₃) = −417.1.²⁶ Because our data for synthetic (+)-**1** matched both the data reported by Rowley¹ and in the Japanese patent,³ we concluded that all three compounds are identical, that is to say one and the same.

For the photolytically induced rearrangement of epoxy ketone **80** to BE-43472B [(+)-**1**] we propose the radical based mechanism shown in Scheme 17. Thus, it is presumed that initial n → π* photoexcitation of **80** forms transient excited state diradical **81**, which suffers homolytic epoxide rupture as shown to generate diradical **82**. The latter possesses an ideal geometry for a 1,4-hydrogen shift (see σ and n orbital arrangement, structure **82-o** in box) as shown in Scheme 17 to give enol **83**, whose facile and spontaneous tautomerization leads to the observed product [(+)-**1**]. The photolytically induced rearrangement of α,β-oxiranyl ketones to conjugated enol ketones was observed as early as 1918 by Bodfoss,²⁹ and recently revisited by Jang, Park, and coworkers³⁰ in a flash laser spectroscopic study that revealed a 1,4-hydrogen shift as a key element of its mechanism.

Having completed the total synthesis of both (+)-**1** and (−)-**1**, we then attempted to construct the C-3 epimer of the natural product [(+)-**1**] starting from the C-3 epimeric enone 3-*epi*-**75**, which we obtained from the SeO₂ mediated oxidation of 9a-*epi*-**72/72** (see Scheme 16). As shown in Scheme 18, selective thioketalization of 3-*epi*-**75** under the previously developed conditions (ethane-1,2-dithiol as solvent, 15 equiv BF₃•OEt₂) gave dithiolane 3-*epi*-**78** in 66% yield. Reductive desulfurization of this compound (Raney-Ni 2400, MeOH; then aq. HCl) furnished enone 3-*epi*-**79** (27% yield, unoptimized), which was subjected to epoxidation (*t*-BuOOH, DBU, −30 °C) to afford β-oxirane 3-*epi*-**80** as a single isomer and in 97% yield. Unfortunately, irradiation of the latter oxirane under the same conditions (benzene, ambient temperature) used for the successful rearrangement of oxirane **80** (see Scheme 17) failed to induce any change, leading only to recovered starting material. This outcome did not change, neither by irradiation in benzene at 60 °C, nor by changing the solvent to MeOH (irradiation

at ambient temperature). Interestingly, we observed the same reluctance of α -oxirane **α-80** (Scheme 17) to undergo the photolytically induced rearrangement to the desired enol structure. These results may be explained by considering the frontier molecular orbitals of the epoxy ketone structural motif in each of the three substrates subjected to the photolytic conditions (**80**, **α-80**, and **3-*epi*-80**), as illustrated in Figure 6. As seen, the structure of the oxiranyl ketone **80** allows almost perfect alignment of the C-9a–O bond and its associated σ^* orbital with the π^* orbital of the adjacent C=O bond as required for the oxirane rupture (see drawing **80-o**, Figure 6). The indicated H-bonding between the C-3 hydroxyl group and the oxirane oxygen [downfield shift of the OH proton to $\delta = 3.37$ ppm in the ^1H NMR spectrum, CDCl_3 , 500 MHz; higher R_f value of oxiranyl ketone **80** (TLC, silica) as compared to that of enone **79**] is presumed to play a subtle role in bringing about this alignment by pulling the oxirane oxygen atom closer to the C-3 hydroxyl group. In contrast to the situation with the β -oxirane **80**, in the C-3 epimeric β -oxirane **3-*epi*-80** the steric repulsion between the C-3 methyl group and the pseudoaxial oxirane moiety results in the bending of the latter out of the required orthogonal geometry to the adjacent carbonyl moiety, resulting in insufficient overlap of the C-9a–O σ^* orbital with the π^* orbital of the carbonyl group for fragmentation to occur (see drawing **3-*epi*-80**, Figure 6). A similar situation exists for the α -oxirane, **α-80** (which could have provided BE-43472B had the epoxide rearrangement occurred) in which the stereoelectronics are even worse (see drawing **α-80-o**, Figure 6). Indeed, the preferred conformation of the *cis*-decalin system within which the epoxy ketone structural motif resides forces the oxirane into an equatorial position, resulting in inadequate orbital overlap between the relevant σ^* and π^* orbitals. Manual molecular modeling is sufficient to recognize these crucial stereoelectronic effects within the oxiranes discussed above.

Biological Evaluation of Both Enantiomers of Antibiotic BE-43472B and Related Compounds

The set of the synthesized compounds enabled us to biologically evaluate a selected number of them in order to obtain insights on structure-activity relationships (SARs) within the class. The results are listed in Table 1 (none of the compounds tested showed activity against *E. Coli* at $100 \mu\text{M}$).

The antimicrobial activities of both enantiomers of the bisanthraquinone BE-43472B [(+)-**1** and (−)-**1**] and analogues thereof were determined against Gram-positive methicillin-resistant *Staphylococcus aureus* (MRSA), vancomycin-resistant *Enterococcus faecalis* (VRE), and Gram negative *Escherichia coli*. In accord with the values reported by Rowley and coworkers^{1,2}, (+)-**1** (natural enantiomer) exhibited strong bactericidal activity against Gram-positive pathogens (MRSA and VRE). Given the architectural complexity of **1** it is notable that the unnatural enantiomer [(−)-**1**] displayed almost similar activity. The fact that all of the derivatives screened in these assay (**55**, **72**, **75**, **3-*epi*-75**, **ent-75**, **ent-3-*epi*-75**, **78**, **ent-3-*epi*-78**, **79**, **ent-79**, **80**, **α-80**, **3-*epi*-79**, **3-*epi*-80**) lack activity implies that the enol functionality (C-1 hydroxyl) is critical for antibacterial activity.

The initial cytotoxicity evaluation of **1** and derivatives thereof was performed across a panel of three cell lines of different histological origin (HCT-116, colon; MCF-7, breast; and HeLa, cervix). It is worth noting that both (+)-**1** and (−)-**1** displayed higher potency against HeLa and HCT-116 cells than against MCF-7 cells. While for HeLa and HCT-116 cells (−)-**1** is slightly more active than its enantiomer (+)-**1**, in the case of MCF-7 cells the (+)-**1** enantiomer exhibited an IC_{50} value almost two times higher than the (−)-**1** enantiomer. Additionally, the simple dienophile **55** (for structure, see Scheme 15) displayed activity in all three tested cell lines with IC_{50} values in the same order of magnitude as (+)-**1** and (−)-**1** (entry 3, 7 μM against HCT-116, 5 μM against HeLa, and 15 μM against MCF-7). While none of the tested compounds exhibited significant antibacterial properties against the bacterial strains employed, a number of them showed notable activities against some, or all, of the tumor cell lines used. Those included

enones **75** (entry 5, 16 μ M against HCT-116 and 18 μ M against HeLa), *3-epi-75* (entry 6, 10 μ M against HCT-116 and 7.7 μ M against HeLa), *ent-3-epi-75* (entry 8, 16 μ M against HCT-116 and 14 μ M against HeLa), *ent-3-epi-78* (entry 10, 31 μ M against HCT-116 and 30 μ M against HeLa), as well as alkenes **79** (entry 11, 32 μ M against HCT-116), *ent-79* (entry 12, 30 μ M against HeLa), and *3-epi-79* (entry 15, 8 μ M against HCT-116, 9 μ M against HeLa, and 40 μ M against MCF-7). The latter compound showed IC₅₀ values against all three cell lines that are reminiscent of the natural product itself despite lacking the C-1 hydroxyl group, which appears to be necessary for the aforementioned antibacterial activity. In addition, it is interesting to note that epoxidation of the C-1/C-9a olefin leads to a complete loss of growth inhibition activity (**72**, **80**, α -**80**, and *3-epi-80*).

These initial investigations into the biology of **1** and related compounds led to the following conclusions: 1) the potencies of the natural and unnatural enantiomers of **1** against bacteria and tumor cells are similar despite their rigid polycyclic, but antipodal structures, 2) antibacterial activity is abolished with even slight modifications of the C-ring of the molecule, and 3) whereas the enol form of the 1,3-dicarbonyl function (C-1 hydroxyl) is critical for antibacterial activity, an α,β -unsaturated carbonyl C-1 hydrogen) is in some cases (i.e. **75**, *3-epi-75*, *ent-3-epi-75*, **79**, *ent-79*, *3-epi-79*) sufficient to retain cytotoxic activity. On the other hand, epoxidation of the enone functionality leads to complete loss of activity.

Conclusion

Based on a cascade sequence, initiated by a thermally induced Diels–Alder reaction, the described synthetic strategy led to an efficient total syntheses of (+)- and (−)-bisanthraquinone antibiotic BE-43472B [(+)-**1** and (−)-**1**] and the assignment of the absolute configuration of this natural product as (+)-**1**. In addition to demonstrating the power of cascade reactions in total synthesis,²⁶ the developed chemistry highlights the use of heat and light as tools for green and efficient chemistry. Biological evaluation of (+)-**1** and (−)-**1** revealed that both compounds are endowed with almost equipotent antibacterial properties and are less active as antitumor agents. Although the various derivatives and intermediates en route to **1** were not as potent antibacterial agents, important information has been gathered from the biological evaluation of these compounds regarding useful structure-activity relationships (SARs) to aid in the design of future analogs. With a synthetic pathway to the BE-43472B structure now available and initial biological data in hand, the design and synthesis of analogues of antibiotic BE-43472B as part of an effort to discover and develop new antibacterial agents is now feasible.

Supplementary Material

Refer to Web version on PubMed Central for supplementary material.

Acknowledgments

Insightful discussions with Prof. A. Eschenmoser regarding the mechanistic aspects of this work are gratefully acknowledged. We thank Prof. D. C. Rowley and A. Socha for a sample of BE-43472B [(+)-**1**]. We also thank Dr. D. H. Huang and Dr. L. Pasterneck, Dr. G. Siuzdak, and Dr. R. Chadha for NMR spectroscopic, mass spectrometric, and X-ray crystallographic assistance, respectively. Financial support for this work was provided by Evonik Industries (Germany), the National Institutes of Health (USA), the National Science Foundation (CHE-0603217), the Skaggs Institute for Chemical Biology, the Alexander von Humboldt Foundation (Germany, postdoctoral fellowship to J.B.), A*STAR (Singapore, predoctoral fellowship to Y.H.L.), the Skaggs-Oxford scholarship program (predoctoral fellowship to Y.H.L.), the NSERC (Canada, postdoctoral fellowship to A.L.), and the Max Weber-Programm (Germany, student internship stipend to T.N.).

References

1. Socha AM, Garcia D, Sheffer R, Rowley DC. *J. Nat. Prod.* 2006;69:1070. [PubMed: 16872146]

2. Socha AM, LaPlante KL, Rowley DC. *Bioorg. Med. Chem* 2006;14:8446. [PubMed: 16979896]
3. Kushida, H.; Nakajima, S.; Koyama, T.; Suzuki, H.; Ojiri, K.; Suda, H. *Antitumoric BE-43472 Manufacture with Streptomyces*. 1996. JP 08143569
4. For selected references, see: a Nicolaou KC, Chen JS, Edmonds DJ, Estrada AA. *Angew. Chem., Int. Ed* 2009;48:660. b Roberts L, Simpson S. *Science* 2008;321:355. [PubMed: 18635787], and references therein. c Walsh CT, Wright G. *Chem. Rev* 2005;105:391. [PubMed: 15700949] d Nicolaou KC, Boddy CNC, Bräse S, Winssinger N. *Angew. Chem., Int. Ed* 1999;38:2096.
5. For previous synthetic studies inspired by BE-43472B, see: a Takikawa H, Hikita K, Suzuki K. *Angew. Chem., Int. Ed* 2008;47:9887. b Suzuki K, Takikawa H, Hachisu Y, Bode JW. *Angew. Chem., Int. Ed* 2007;46:3252.
6. For a preliminary communication on this work, see: Nicolaou KC, Lim YH, Becker J. *Angew. Chem., Int. Ed* 2009;48:3444.
7. Highlight: Rowley DC. *Nature Chemistry* 2009;1:110.
8. Nicolaou KC, Lim YH, Piper JL, Papageorgiou CD. *J. Am. Chem. Soc* 2007;129:4001. [PubMed: 17355133]
9. Nicolaou KC, Lim YH, Papageorgiou CD, Piper JL. *Angew. Chem., Int. Ed* 2005;44:7917.
10. Reviews: a Snieckus V. *Chem. Rev* 1990;90:879. b Whisler MC, MacNeil S, Snieckus V, Beak P. *Angew. Chem., Int. Ed* 2004;43:2206.
11. a Hauser FM, Rhee RP. *J. Org. Chem* 1978;43:78. b Hauser FM, Chakrapani S, Ellenberger WP. *J. Org. Chem* 1991;56:5248. c Mal D, Ray S, Sharma I. *J. Org. Chem* 2007;72:4981. [PubMed: 17511506]. Review: d Mal D, Pahari P. *Chem. Rev* 2007;107:1892. [PubMed: 17444689]
12. For Diels–Alder reactions with juglone as dienophile, see: a Trost BM, Ippen J, Vladuchick WC. *J. Am. Chem. Soc* 1977;99:8116. b Stork G, Hagedorn AA III. *J. Am. Chem. Soc* 1978;100:3609. c Boeckman RK Jr, Dolak TM, Culos KO. *J. Am. Chem. Soc* 1978;100:7098.
13. The synthesis of dienes **33a** and **33b** was inspired by the work of McDougal et al., see: a McDougal PG, Jump JM, Rojas C, Rico JG. *Tetrahedron Lett* 1989;30:3897. b McDougal PG, Rico JG. *J. Org. Chem* 1987;52:4817.
14. Denmark SE, Jones TK. *J. Org. Chem* 1982;47:4595.
15. Review: a Fürstner A. *Chem. Rev* 1999;99:991. [PubMed: 11848998] For an example where the Z-iodoalkene retains its stereochemistry after coupling, see: b Nicolaou KC, Baran PS, Zhong Y-L, Barluenga S, Hunt KW, Kranich R, Vega JA. *J. Am. Chem. Soc* 2002;124:2233. [PubMed: 11878977]
16. Overman LE, Rishton GM. *Org. Synth., Coll* 1998;IX:139. Overman LE, Rishton GM. *Org. Synth* 1993;71:56.
17. Isomers **32a** and **32b** exhibited similar reactivities in this elimination reaction on exposure to *s*-BuLi as noted in their reactions either as individual compounds, or as a mixture. Partial elimination of MeOH from the terminal MEM group of diene **33a** to form the corresponding triene was observed on prolonged reaction times or when excessive amounts of base were used.
18. Reviews: a Farina, V.; Krishnamurthy, V.; Scott, WK. *Org. React.* Vol. 50. Wiley-VCH; New York: 1997. p. 1 b Fugami K, Kosugin M. *Top. Curr. Chem* 2002;219:1.c Mitchell, TN. *Metal-Catalyzed Cross-Coupling Reactions*. Vol. 2nd. ed.. de Meijere, A.; Diederich, F., editors. Wiley-VCH; Weinheim: 2004. p. 125
19. Echavarren AM, Tamayo N, Cárdenas DJ. *J. Org. Chem* 1994;59:6075.
20. Grunwell JR, Karipides A, Wigal CT, Heinzman SW, Parlow J, Surso JA, Clayton L, Fleitz FJ, Daffner M, Stevens JE. *J. Org. Chem* 1991;56:91.
21. a Tietze LF, Gericke KM, Singidi RR, Schuberth I. *Org. Biomol. Chem* 2007;5:1191. [PubMed: 17406717] b Boeckman RK Jr, Dolak TM, Culos KO. *J. Am. Chem. Soc* 1978;100:7098. c Kelly TR, Montury M. *Tetrahedron Lett* 1978;45:4311. d Trost BM, Ippen J, Vladuchick WC. *J. Am. Chem. Soc* 1977;99:8116.
22. For Diels–Alder reactions with similar chiral 1,3-dienes, see: a Barriault L, Thomas JDO, Clément R. *J. Org. Chem* 2003;68:2317. [PubMed: 12636397] b Carreño MC, Garcíá-Cerrada S, Urbano A, Di Vitta C. *J. Org. Chem* 2000;65:4355. [PubMed: 10891138]. (c) Ref. 12(a).
23. Rozeboom MD, Tegmo-Larsson I-M, Houk KN. *J. Org. Chem* 1981;46:2338.

24. Marshall JA, Yanik MM, Adams ND, Ellis KC, Chobanian HR. Org. Synth 2005;81:157.
25. a Nahm S, Weinreb SM. Tetrahedron Lett 1981;22:3815. b Sibi MP. Org. Prep. Proced. Int 1993;25:15. c Mentzel M, Hoffmann HMR. J. Prakt. Chem 1997;339:517. d Singh J, Satyamurthi N, Aidhen IS. J. Prakt. Chem 2000;342:340.
26. Reviews: a Nicolaou KC, Edmonds DJ, Bulger PG. Angew. Chem. Int. Ed 2006;45:7134.b Tietze, LF.; Brasche, G.; Gericke, K. Domino Reactions in Organic Synthesis. Wiley-VCH: Weinheim: 2006. p. 672 c Nicolaou KC, Montagnon T, Snyder SA. Chem. Commun 2003:551.
27. Since epimers **72** and *epi*-**72** are hardly separable and because the subsequent intermediates **73** and **74** were also shown to epimerize under the reaction conditions employed for their generation, it was more expedient and efficient to carry the mixture of **72** and *epi*-**72** through the three-step sequence and separate the obtained enones (**75** and its C-3 epimer *epi*-**75**) by chromatography.
28. Tsuji J, Nagashima H, Hori K. Chem. Lett 1980:257.
29. Bodforss S. Ber. deut. chem. Ges 1918;51:214. b Jeger O, Schaffner K. Pure Appl. Chem 1970;21:247. [PubMed: 5458819]
30. Kim H, Kim TG, Hahn J, Jang D-J, Chang DJ, Park BS. J. Phys. Chem. A 2001;105:3555.

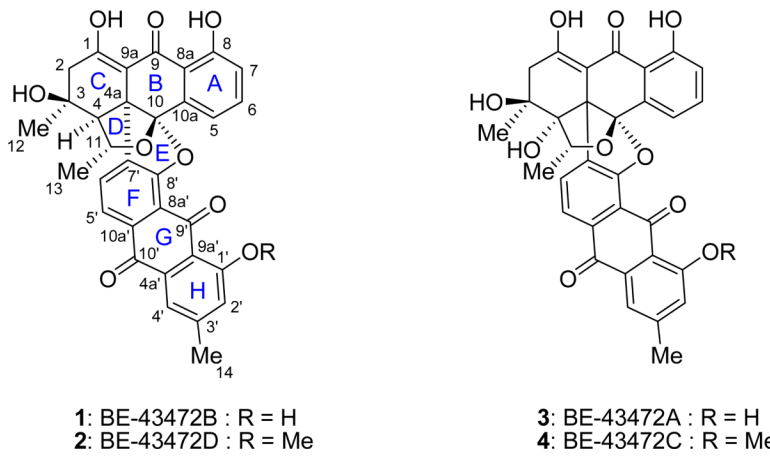
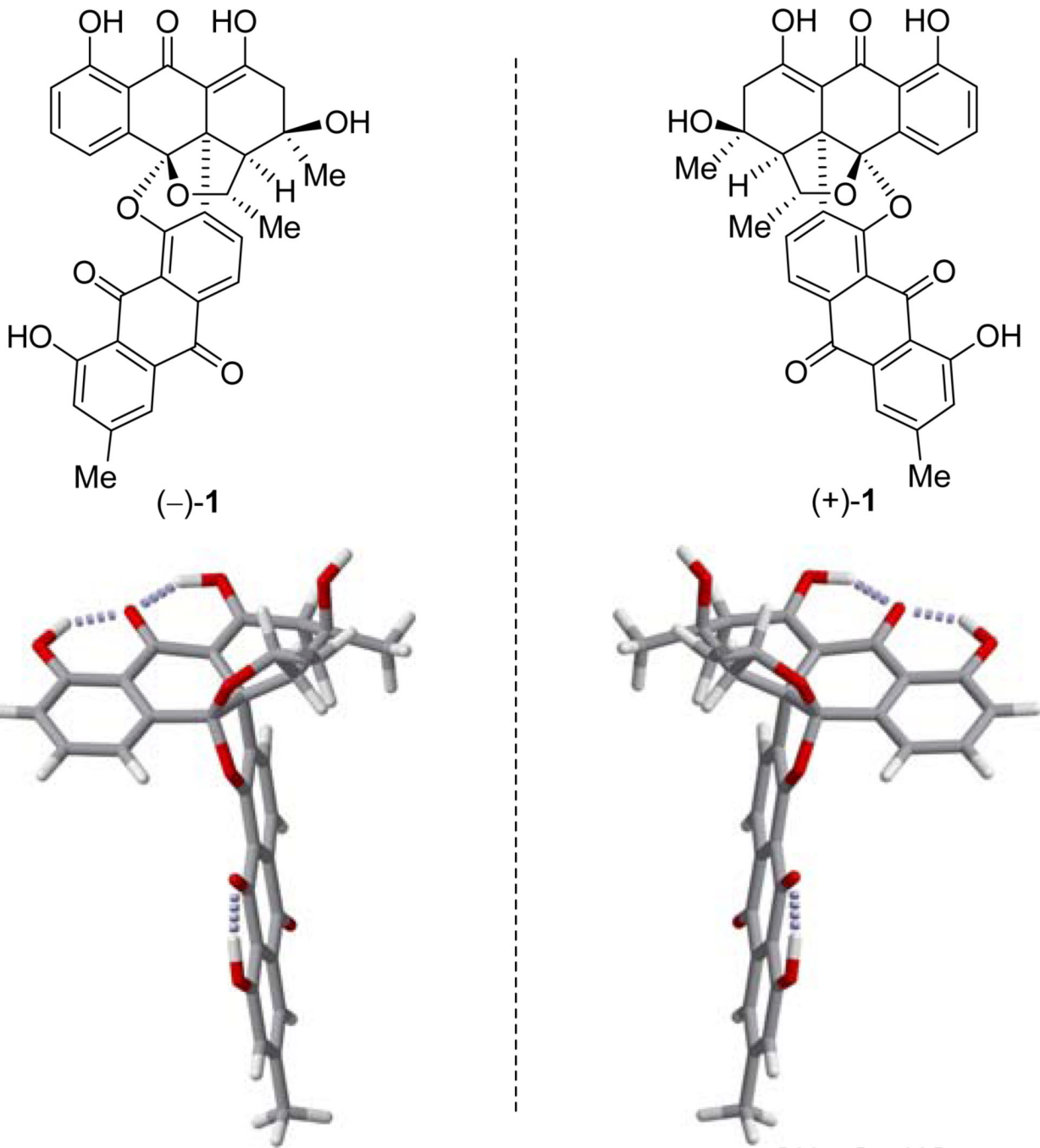
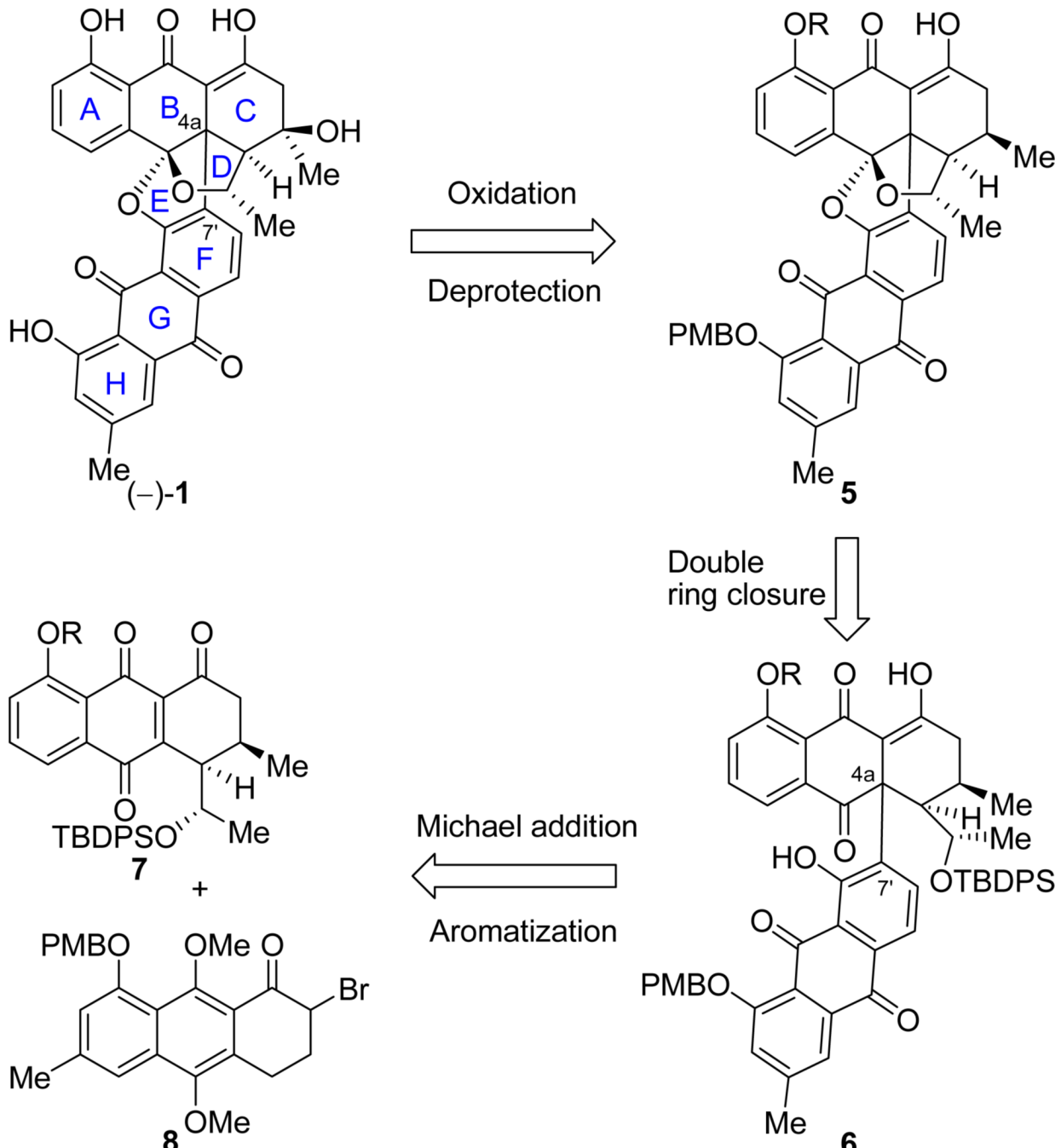


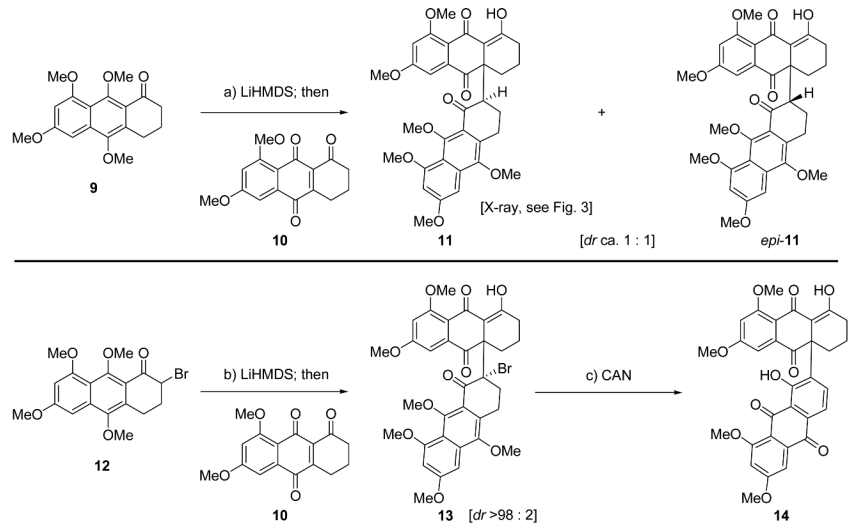
Figure 1.
Bisanthraquinone antibiotics BE-43472A–D (**1–4**).

**Figure 2.**

Enantiomers of bisanthraquinone antibiotic BE-43472B [(-)-1 and (+)-1] (top) and their computer-generated molecular models (bottom, fully optimized at the B3LYP/6-31G* level, Spartan '06 suite of programs, carbon: gray, hydrogen: white, oxygen: red, H-bonds: dotted gray).



Scheme 1.
Initial Retrosynthetic Analysis of Bisanthraquinone ($-$ -1)



^a Reagents and conditions: (a) **9** (1.0 equiv), LiHMDS (1.0 equiv), THF, -78 °C, 2 h, then **10** (1.05 equiv), 15 min, quant. (**11**:*epi*-**11** ca. 1:1); (b) **12** (1.0 equiv), LiHMDS (1.0 equiv), THF, -78 °C, 15 min, then **10** (1.1 equiv), 30 min, -78 → 25 °C, 1.5 h, 63%; (c) CAN (2.2 equiv), MeCN/H₂O (2:1), 0 °C, 30 min, then CAN (1.5 equiv), 30 min, 93%.

Scheme 2.

Initial Model Studies. Investigation of the Key Michael Reaction Step^a

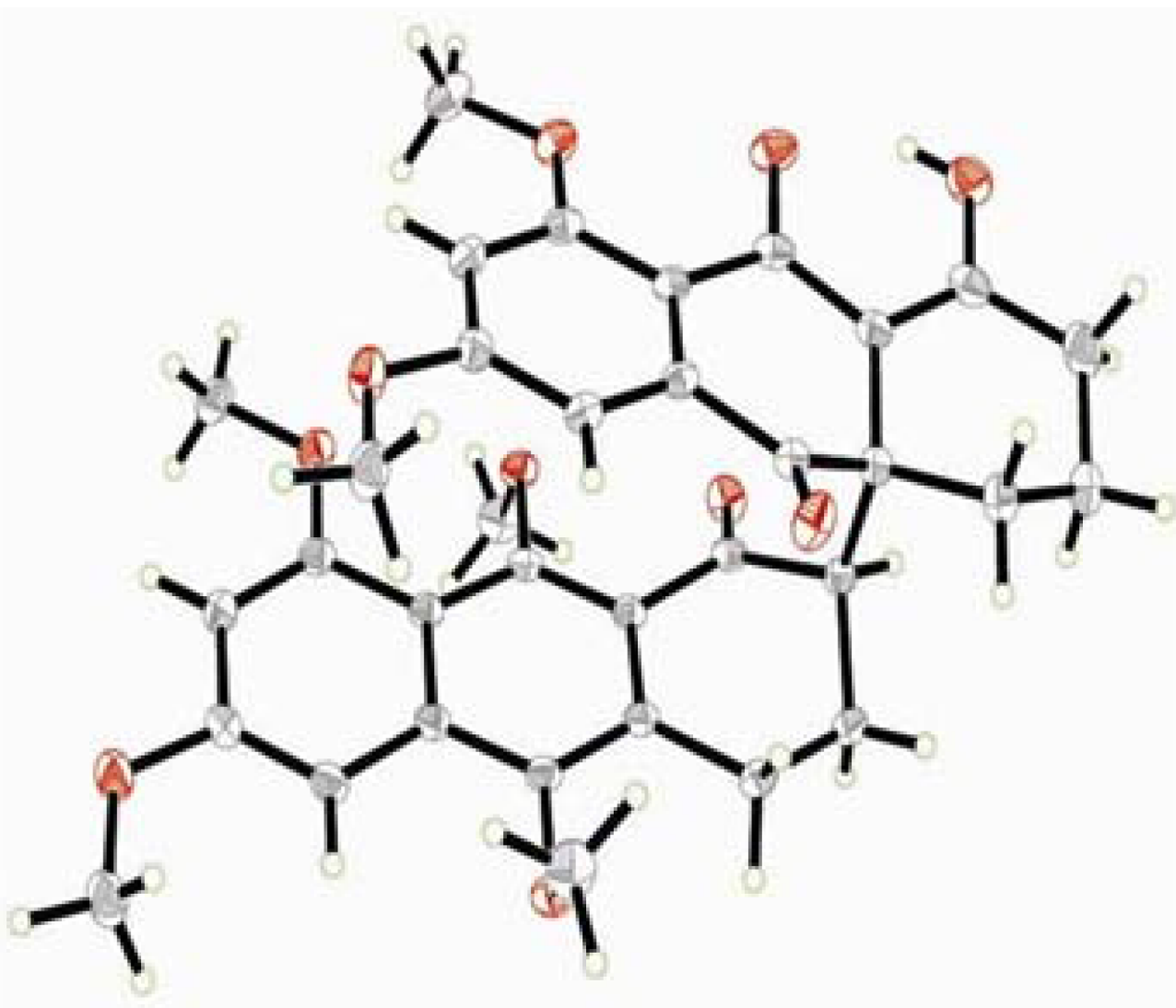
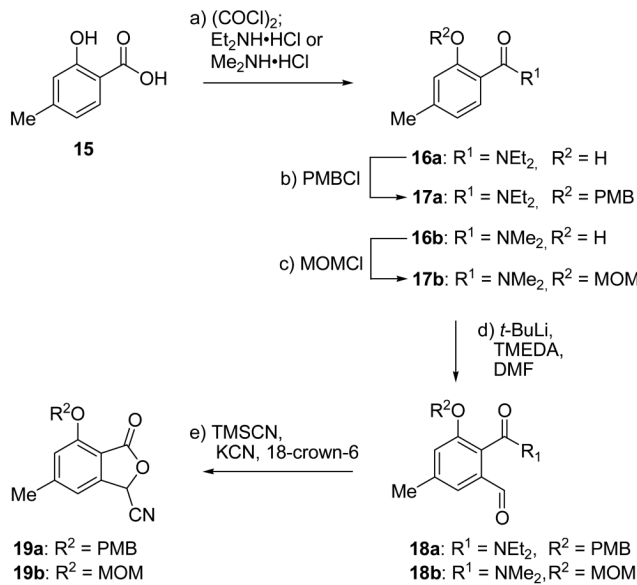
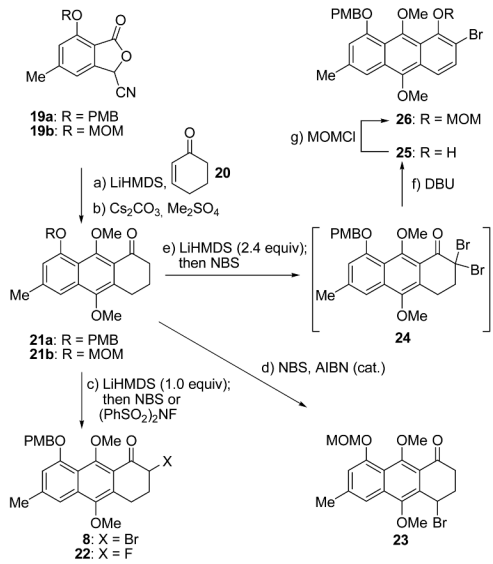


Figure 3.
X-Ray derived ORTEP drawing of compound 11.



^a Reagents and conditions: (a) (COCl)₂ (1.2 equiv), DMF (catalytic), CH₂Cl₂, 0 °C, 30 min, 25 °C, 6 h, then Et₂NH•HCl or Me₂NH•HCl (1.3 equiv), Et₃N (3.0 equiv), CH₂Cl₂ or THF, 0 → 25 °C, 12 h, 74% (**16a**), 88% (**16b**); (b) PMBCl (1.08 equiv), K₂CO₃ (1.5 equiv), TBAI (0.025 equiv), acetone, reflux, 48 h, 99%; (c) MOMCl (1.1 equiv), *i*-Pr₂NEt (1.2 equiv), DMF, 60 °C, 48 h, 97%; (d) TMEDA (2.5 equiv), *t*-BuLi (2.5 equiv), THF, -78 °C, then **17a** (1.0 equiv) or **17b** (1.0 equiv), 1 h, then DMF (3.0 equiv), 30 min, 25 °C, 2 h, 67% (**18a**), 95% (**18b**); (e) KCN (0.2 equiv), 18-crown-6 (0.2 equiv), TMSCN (1.4 equiv), 0 °C, 3 h, then AcOH, 25 °C, 12 h, 76% (**19a**), 85% (**19b**).

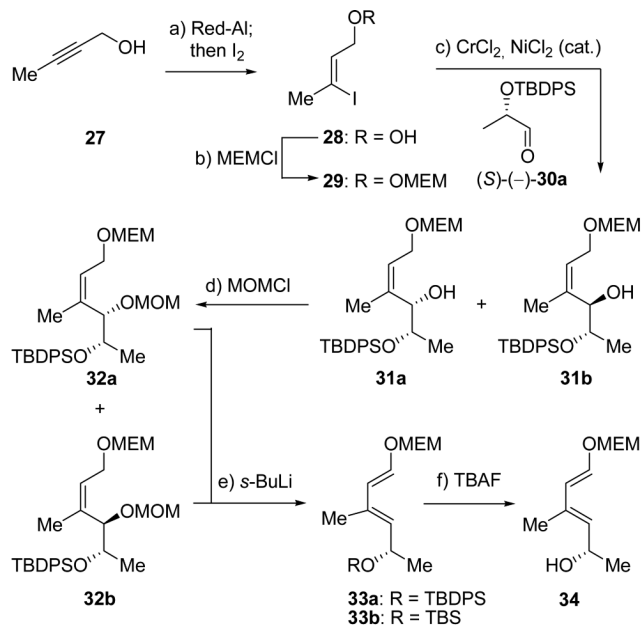
Scheme 3.
Synthesis of Nitriles **19a** and **19b**^a



^a Reagents and conditions: (a) **19a** or **19b** (1.0 equiv), LiHMDS (1.1 equiv), -78 °C, 2 h, then **20** (1.1 equiv), -78 → 25 °C, 18 h; (b) Me_2SO_4 (3.0 equiv), Cs_2CO_3 (3.3 equiv), acetone, reflux, 12 h, 37% (**21a**) from **19a**, 59% (**21b**) over the two steps; (c) LiHMDS (1.0 equiv), THF, -78 °C, 1 h, then NBS (1.0 equiv) or $(\text{PhSO}_2)_2\text{NF}$ (1.05 equiv), 1–1.5 h, 51% (**8**), 98% (**22**); (d) NBS (1.05 equiv), AIBN (0.1 equiv), benzene, 70 °C, 15 min, then AIBN (0.1 equiv), 1 h, 52%; (e) LiHMDS (2.4 equiv), THF, -78 °C, 1 h, then NBS (2.0 equiv), 1.5 h; (f) DBU (1.2 equiv), -78 → 25 °C, 10 h; (g) MOMCl (2.5 equiv), Cs_2CO_3 (2.5 equiv), DMF, 0 → 25 °C, 10 h, 28% over the three steps.

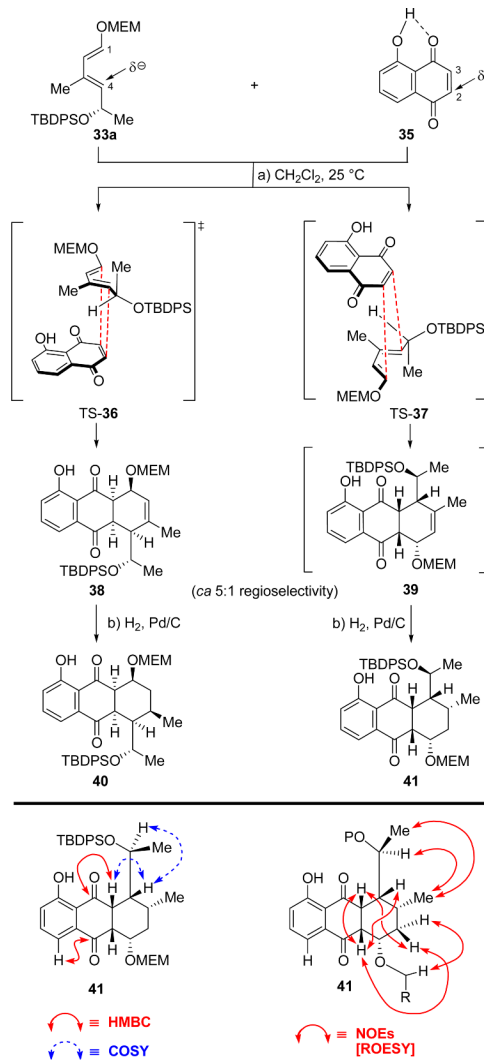
Scheme 4.

Synthesis of Aryl Fragments **8**, **21**, **22**, **23**, and **26**^a



^a Reagents and conditions: (a) Red-Al (1.3 equiv), Et₂O, -78 → 25 °C, 24 h, then I₂ (1.5 equiv), -78 → 25 °C, 4 h; (b) MEMCl (1.8 equiv), *i*-Pr₂NEt (2.2 equiv), CH₂Cl₂, -20 → 25 °C, 18 h, 88% over the two steps; (c) CrCl₂ (3.0 equiv), NiCl₂ (0.04 equiv), then **29** (1.0 equiv), (S)-(-)-**30a** (1.05 equiv), DMF, 0 → 25 °C, 12 h, 90% (**31a**:**31b** ca. 4 : 1); d) MOMCl (1.7 equiv), *i*-Pr₂NEt (1.9 equiv), CH₂Cl₂, 18 h, 91% (**32a**), 90% (**32b**); (e) *s*-BuLi (1.3 equiv), THF, -78 °C, 2 h, 76% (from **32a**:**32b** ca. 4:1); (f) TBAF (1.5 equiv), THF, 25 °C, 16 h, 94%.

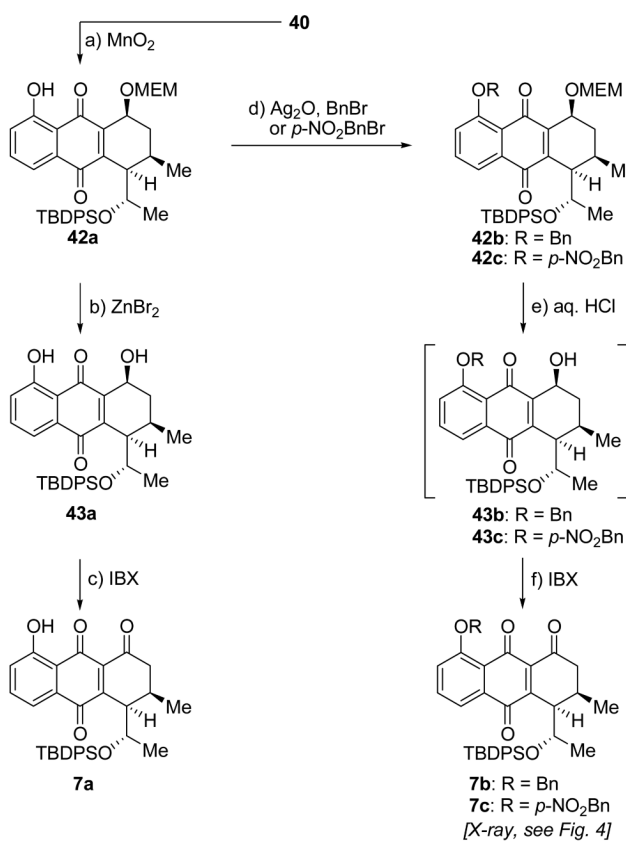
Scheme 5.
Synthesis of Dienes **33** and **34**^a



^a Reagents and conditions: (a) **33a** (1.0 equiv), **35** (1.3 equiv), CH_2Cl_2 , 25°C , 48 h, 81% (**38:39** ca. 5:1); (b) H_2 , 10% Pd/C (20 mol%), MeOH, 59% (**40**) and 15% (**41**) starting from **33a**.

Scheme 6.

Diels–Alder Reaction of Diene **33a** with Juglone (**35**) and Subsequent Hydrogenation^a



^a Reagents and conditions: (a) MnO_2 (10 wt. equiv), CH_2Cl_2 , 25 °C, 24 h, 88%; (b) ZnBr_2 (6.0 equiv), CH_2Cl_2 , 25 °C, quant.; (c) IBX (1.2 equiv), MeCN , 50 °C, 16 h, 94%; (d) RBr (3.0–4.2 equiv), Ag_2O (4.2–5.6 equiv), DMF , 25 °C, 2–4 h, 86% (**42b**), quant. (**42c**); (e) 1% HCl , MeOH , 50 °C, 4–6 h; (f) IBX (1.4 equiv), MeCN , 50 °C, 4–8 h, 89% (**7b**), 78% (**7c**), over the two steps.

Scheme 7.
Synthesis of Quinones **7a–c**^a

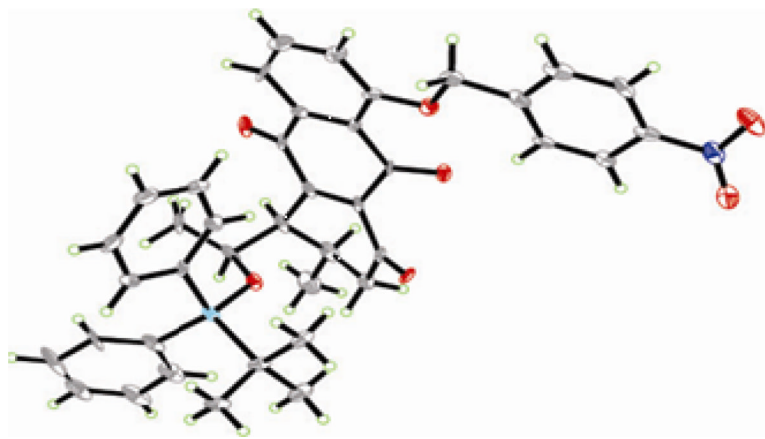
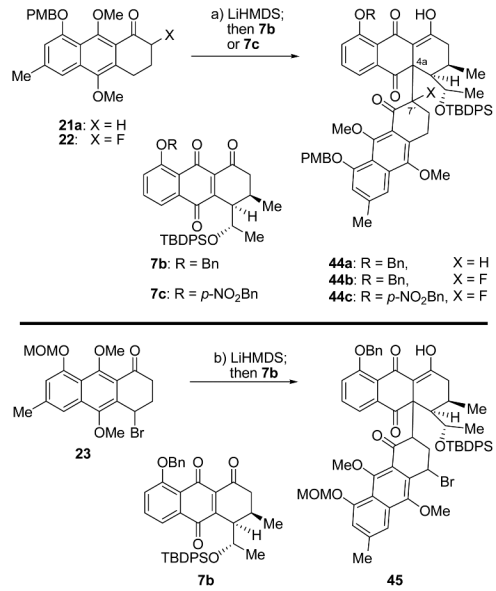


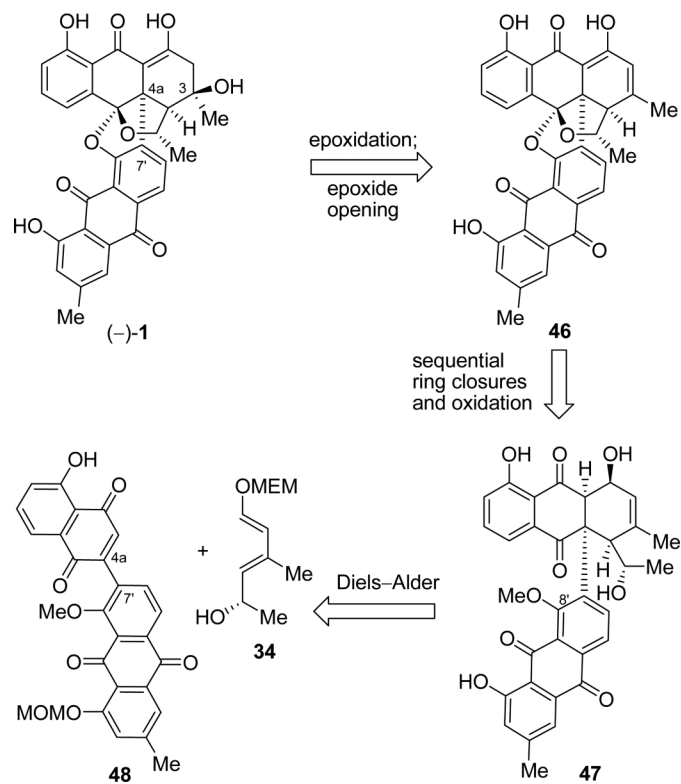
Figure 4.
X-Ray derived ORTEP drawing of quinone **7c**.



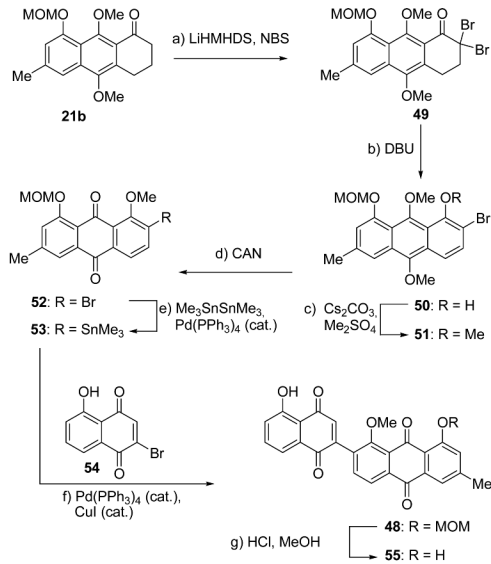
^a Reagents and conditions: (a) for **44a**: **21a** (1.0 equiv), LiHMDS (1.1 equiv), THF, –78 °C, 1 h, then **7b** (1.0 equiv), 30 min, 25 °C, 1.5 h, 31%; for **44b** or **44c**: **22** (1.0 equiv), LiHMDS (1.0 equiv), THF, –78 °C, then **7b** or **7c** (1.0 equiv), B(*n*-Bu)₂OTf (1.0 equiv), –78 → 25 °C, 2 h, 11% (**44b**, *dr* ca. 1:1), 9% (**44c**, *dr* ca. 1:1); (b) **23** (1.0 equiv), LiHMDS (1.06 equiv), THF, –78 °C, 15 min, then **7b** (1.0 equiv), –78 → 0 °C, 1 h, 49% (*dr* ca. 1:1).

Scheme 8.

Michael Reaction/Aromatization Attempts To Construct the Crowded Quaternary C–C Bond^a

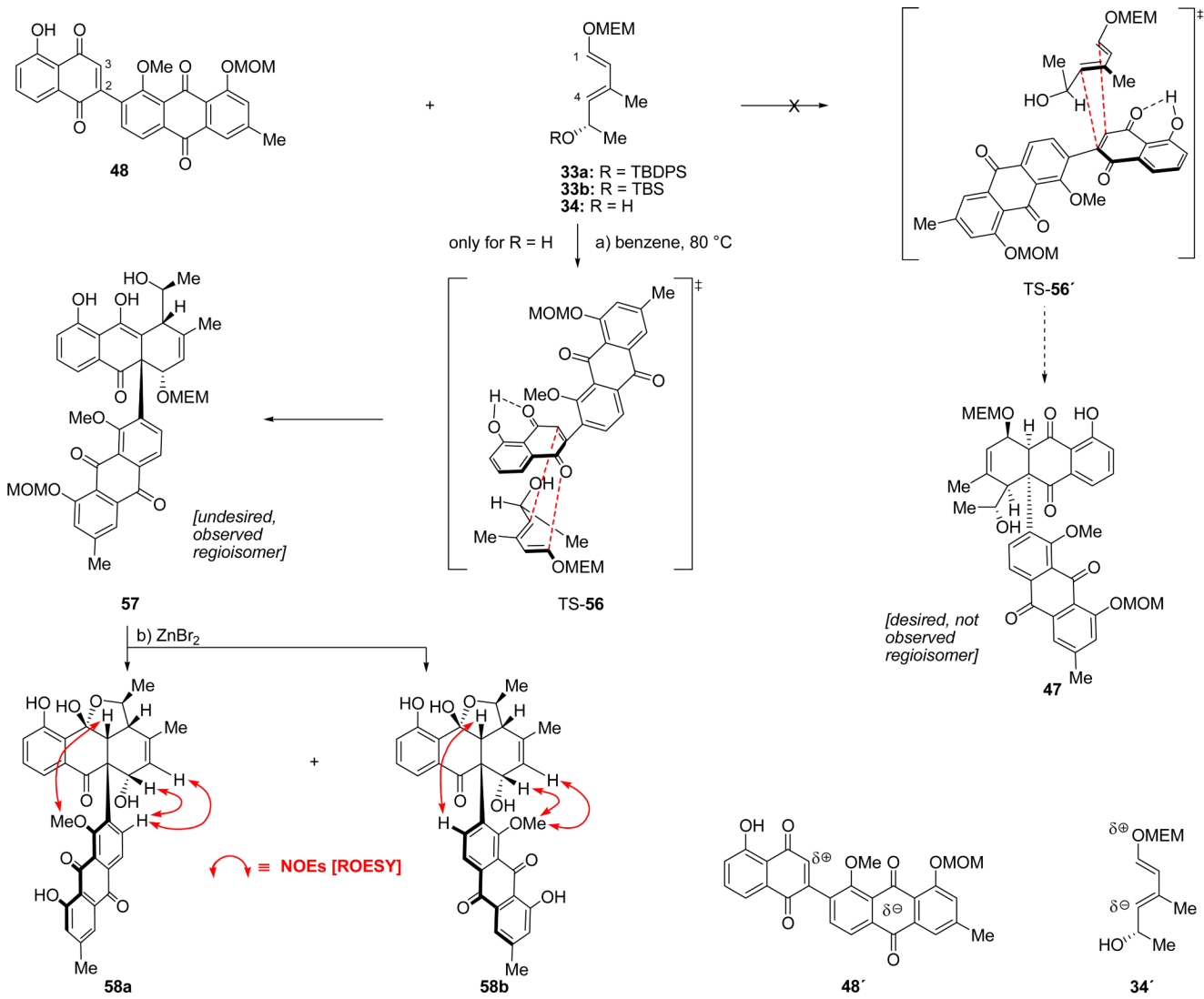
**Scheme 9.**

Second Generation Retrosynthetic Analysis of *(-)*-BE-43472B [*(-)*-1]. The Diels–Alder Approach



^a Reagents and conditions: (a) LiHMDS (2.2 equiv), NBS (2.2 equiv), THF, 0 → 25 °C, 1 h, 98%; (b) DBU (1.0 equiv), CH₂Cl₂, 25 °C, 12 h; (c) Me₂SO₄ (1.2 equiv), Cs₂CO₃ (1.2 equiv), acetone, reflux, 5 h, 74% over the two steps; (d) CAN (2.0 equiv), CH₂Cl₂, MeCN, H₂O, 0 °C, 30 min, 77%; (e) Pd(PPh₃)₄ (0.1 equiv), Me₃SnSnMe₃ (1.5 equiv), toluene, 110 °C, 2 h, 94%; (f) 53 (1.0 equiv), 54 (1.5 equiv), Pd(PPh₃)₄ (0.1 equiv), CuI (0.2 equiv), THF, 70 °C, 22 h, 65%; (g) 1% HCl in MeOH, CH₂Cl₂, 25 °C, 16 h, 85%.

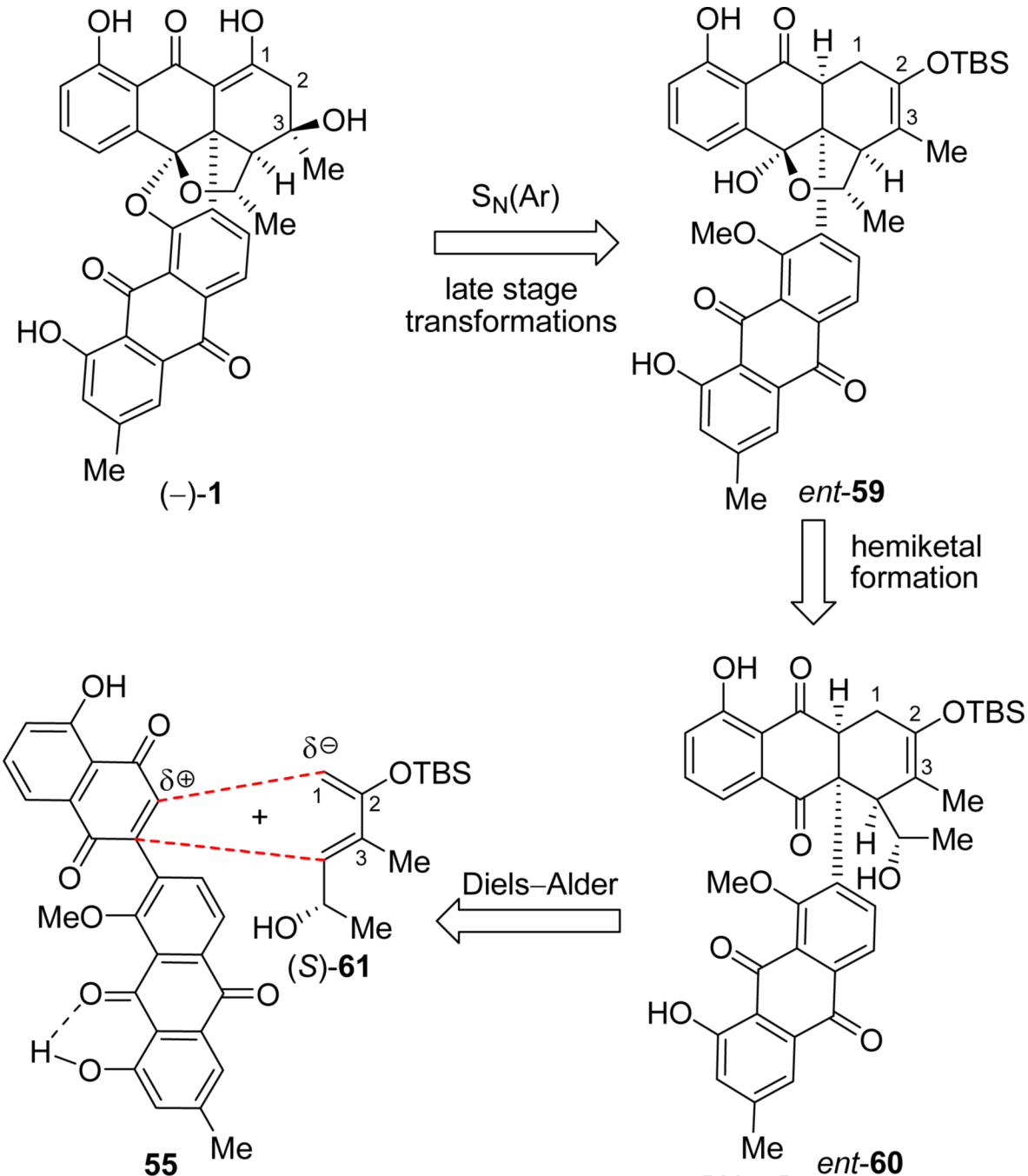
Scheme 10.
Construction of Quinone Dienophiles **48** and **55**^a



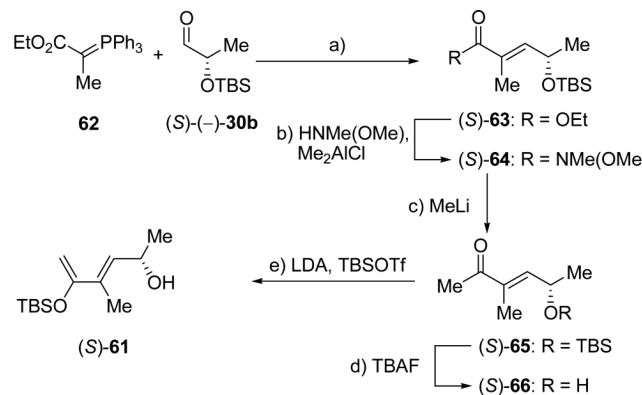
^a Reagents and conditions: (a) **48** (1.0 equiv), **34** (4.0 equiv), benzene, 80 °C, 72 h, 77%; (b) ZnBr₂ (5.0 equiv), CH₂Cl₂, 25 °C, 24 h, 84% (**58a**:**58b** ca. 1:1).

Scheme 11.

Diels–Alder Reaction of Diene **34** with Dienophile **44** Leading to Undesired Regioisomeric Adduct **57** and Atropisomers **58a** and **58b**^a

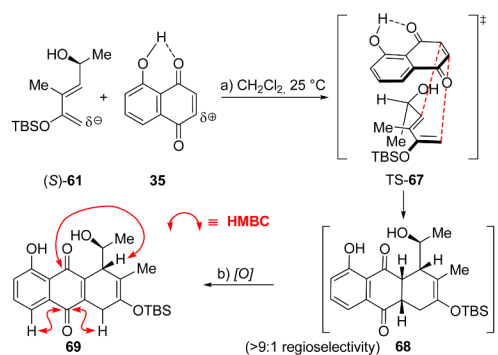


Scheme 12.
Final Retrosynthetic Analysis of *(-)*-BE-43472B [*(-)*-1]



^a Reagents and conditions: (a) (S)-(-)-**30b** (1.0 equiv), **62** (1.1 equiv), CH₂Cl₂, 25 °C, 6 h, 92%; (b) HN(OMe)•HCl (5.0 equiv), Me₂AlCl (5.0 equiv), CH₂Cl₂, 0 → 25 °C, 20 h; (c) MeLi, (2.0 equiv), Et₂O, -78 °C, 1 h, 77% over the two steps; d) TBAF (1.1 equiv), THF, 25 °C, 3 h, 93%; e) LDA (2.3 equiv), THF, -78 °C; then TBSOTf (1.0 equiv), -78 °C, 1.5 h, -78 → 25 °C, 30 min, 33% (95% ee), plus 47% recovered starting material.

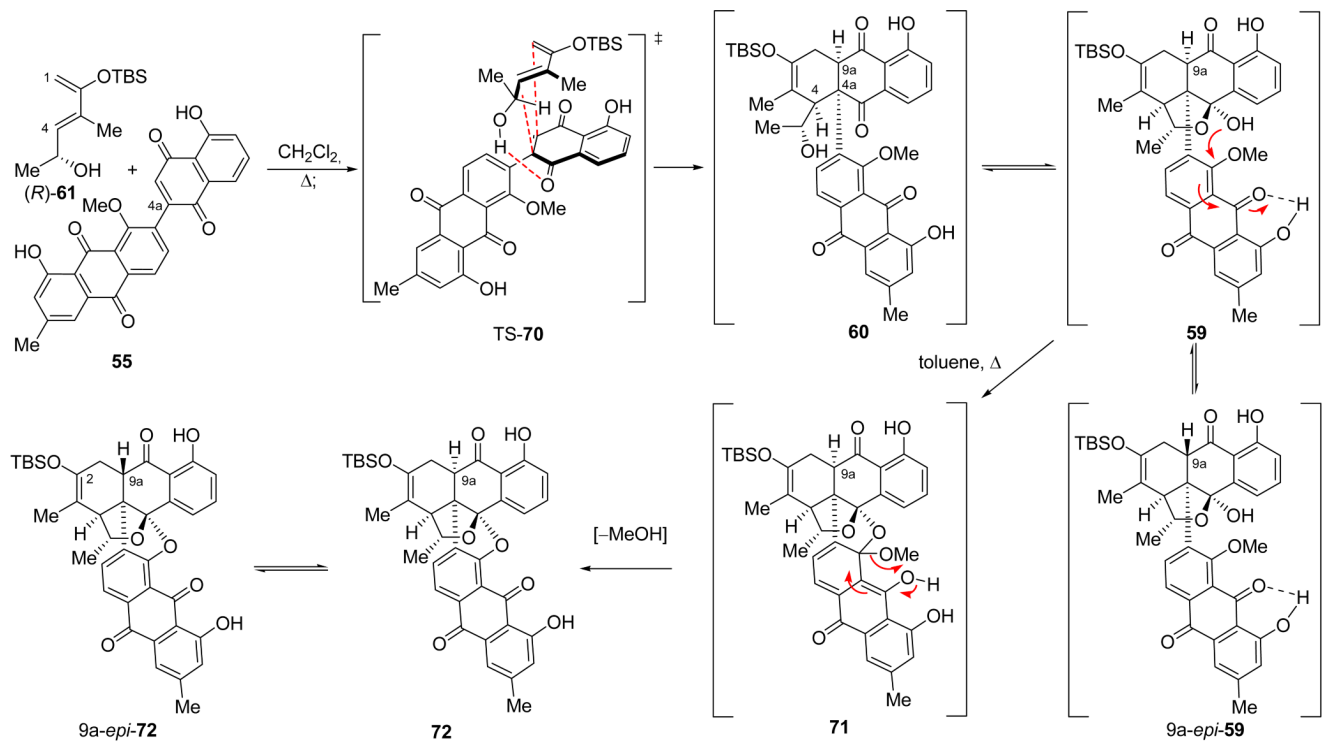
Scheme 13.
Synthesis of Diene (*S*)-**61**^a



^a Reagents and conditions: (a) **35** (1.0 equiv), **(S)-61** (1.1 equiv), 25 °C, 5 h; (b), air, SiO_2 , 25 °C, 30 min, 62% over the two steps.

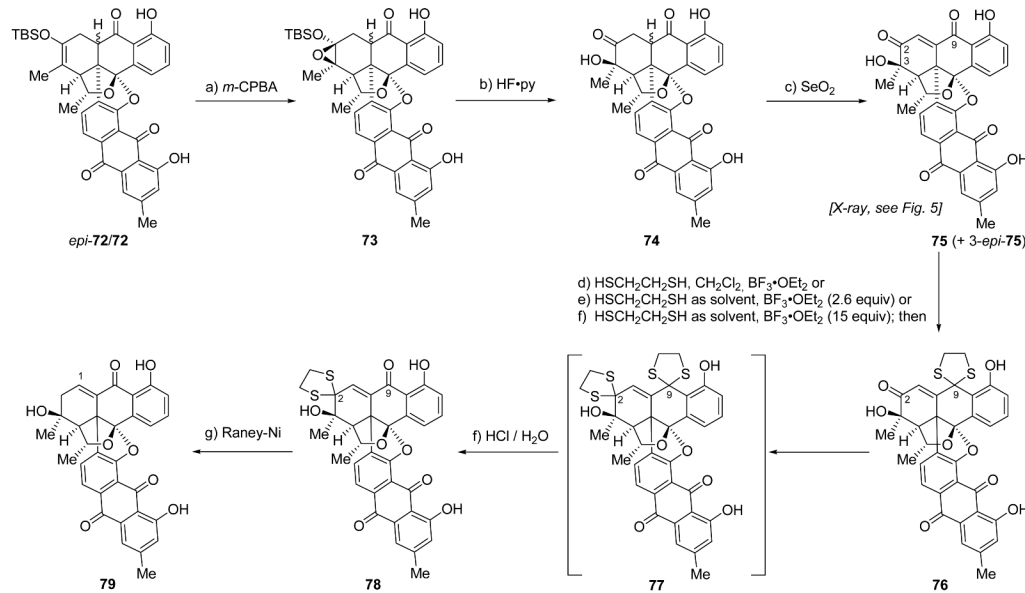
Scheme 14.

Diels–Alder Model Study with Diene *(S)*-61 and Juglone (**35**)^a



^a Reagents and conditions: **55** (1.0 equiv), (*R*)-**61** (2.0 equiv), CH_2Cl_2 , 85 °C, sealed tube, 48 h; then toluene, 135°C, dean stark, 24 h, 9a-*epi*-**72**:**72** (ca. 2:1 mixture of epimers) 98% overall yield based on **55**.

Scheme 15.
Diels–Alder Reaction/Double THF Cyclization Cascade^a



^a Reagents and conditions: (a) $m\text{-CPBA}$ (1.2 equiv), CH_2Cl_2 , -20°C , 2 h; (b) $\text{HF}\text{-py}$ (10.0 equiv), THF, 25°C , 20 min; then TMSOMe ; (c) SeO_2 (5.0 equiv), AcOH , 120°C , 15 h, 49% (**75**) and 39% (3-*epi*-**75**), over the three steps, chromatographically separated; (d) $\text{HSCH}_2\text{CH}_2\text{SH}$ (4.0 equiv), $\text{BF}_3\text{-OEt}_2$ (6.0 equiv), CH_2Cl_2 , 25°C , 28 h, 55% (*ent*-**76**); (e) $\text{HSCH}_2\text{CH}_2\text{SH}$ as solvent, $\text{BF}_3\text{-OEt}_2$ (2.6 equiv), 25°C , 20 min, 78% (*ent*-**76**); (f) $\text{HSCH}_2\text{CH}_2\text{SH}$ as solvent, $\text{BF}_3\text{-OEt}_2$ (15 equiv), 25°C , 30 min; then 0.1 M HCl , 63% (**78**); (g) Raney-Ni 2400, MeOH , air, 25°C , 1.5 h, then aq. HCl , 45% (plus 19% recovered starting material, 56% yield of **79** brsm).

Scheme 16.

Late Stage Functional Group Transformations and Synthesis of Enone **79**^a

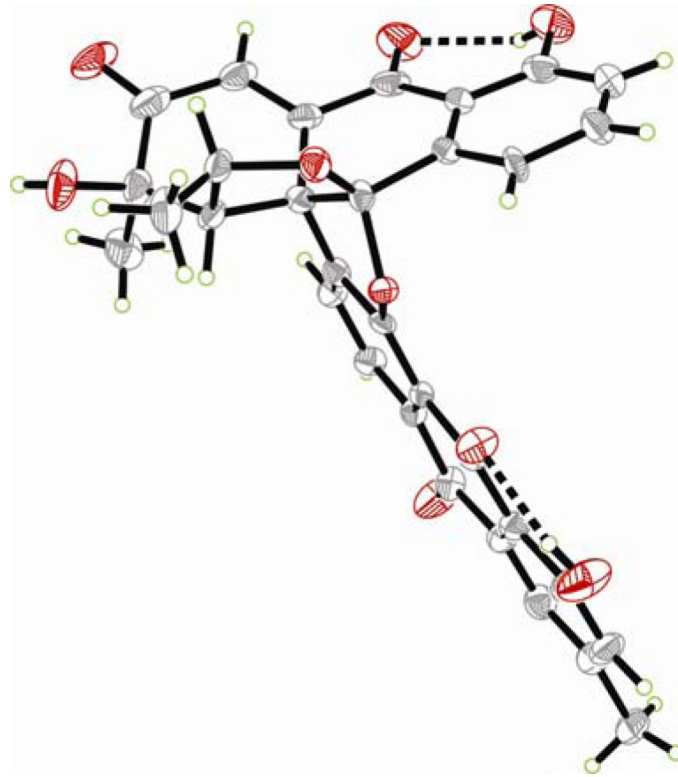
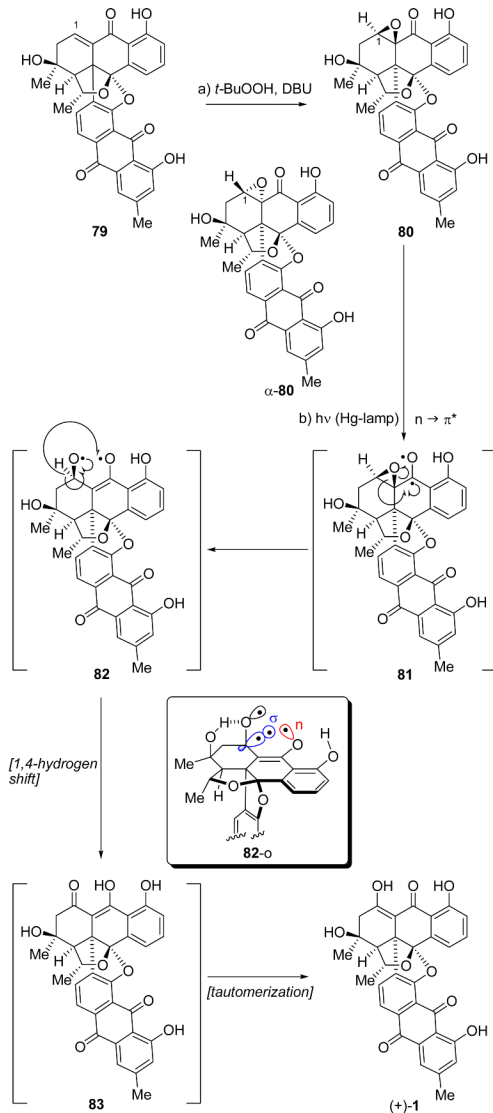
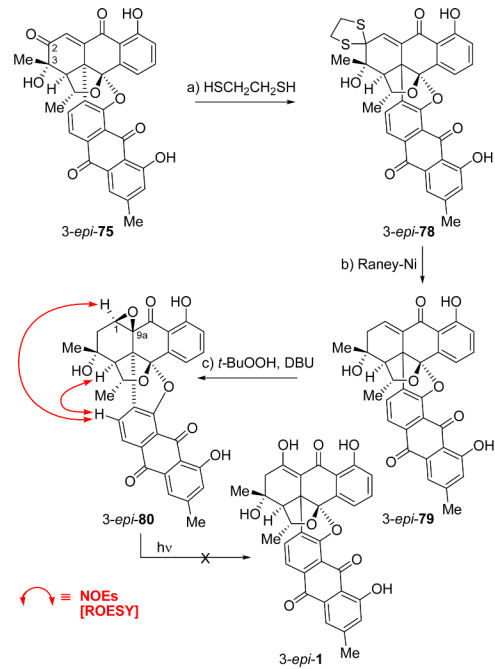


Figure 5.
ORTEP drawing of enone **75** derived from X-ray crystallographic analysis.



^a Reagents and conditions: (a) *t*-BuOOH (5.0 equiv), DBU (3.0 equiv), CH_2Cl_2 , -25°C , 84% (**80**) and, 7% (α -**80**); (b) hv (mercury lamp), benzene, 25°C , 7 h, 77% (83% yield based on 92% conversion).

Scheme 17.
Final Steps of the Total Synthesis of BE-43472B [(+)-1]^a



^a Reagents and conditions: (a) HSCH₂CH₂SH, as solvent, BF₃•OEt₂ (15 equiv), 25 °C, 30 min, 66%; (b) Raney-Ni 2400, MeOH, air, 25 °C, 2 h, then aq. HCl, 3-*epi*-79, 27%; (c) t-BuOOH (5.0 equiv), DBU (3.0 equiv), CH₂Cl₂, –30 °C, 97%.

Scheme 18.

Synthesis of the C-3 Epimeric Oxirane 3-*epi*-80 and Attempted Photolytic Rearrangement^a

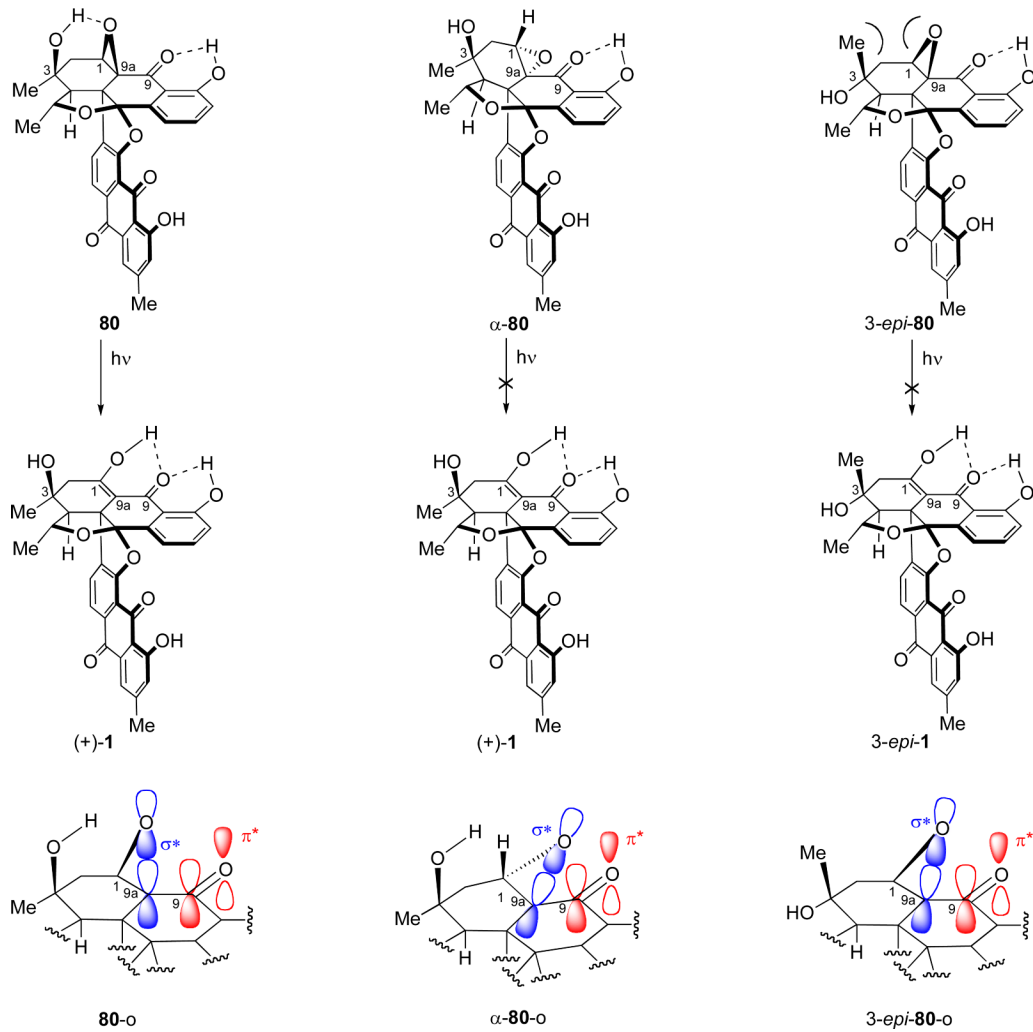


Figure 6.
Conformations of the diastereomeric oxiranes **80**, **α -80**, and **3-epi-80** (oxirane orbitals are shown on a straight line for convenience).

Table 1

Biological Activities of (+)- and (-)-BE-43472B and Related Compounds

Entry	Compound	MRSA ^b	MIC (μ M) ^a	VRE ^c	HCT-116 ^e	IC ₅₀ (μ M) ^d	HeLa ^f	MCF-7 ^g
1	(+)-1	0.15–0.3	0.6–1.5	4.1	2.6	26		
2	(-)-1	0.10–0.2	0.3–2.0	3.8	2.2	40		
3	55	NA	NA	7	5	15		
4	72	NA	NA	NA	NA	NA		
5	75	NA	NA	NA	16	18		
6	3- <i>epi</i> -75	NA	NA	NA	10	7.7		
7	ent-75	NA	NA	NA	NA	NA		
8	ent-3- <i>epi</i> -75	NA	NA	NA	NA	NA		
9	78	NA	NA	NA	NA	NA		
10	ent-3- <i>epi</i> -78	NA	NA	NA	NA	NA		
11	79	NA	NA	NA	NA	NA		
12	ent-79	NA	NA	NA	NA	NA		
13	80	NA	NA	NA	NA	NA		
14	α-80	NA	NA	NA	NA	NA		
15	3- <i>epi</i> -79	NA	NA	NA	NA	NA		
16	3- <i>epi</i> -80	NA	NA	NA	NA	NA		

NA: Not active at the highest concentration tested (100 μ M for the antibacterial assay and 40 μ M for the cytotoxicity assay). (Further information is available in the supplementary information).^aMinimum Inhibitory Concentration.^bMethicillin-resistant *Staphylococcus aureus*.^cVancomycin-resistant *Enterococcus faecalis*.^dConcentration that causes 50% of cell growth inhibition. Experiments were done in triplicates as described in the supplementary information.^eHuman colon cancer cell line.^fHuman cervical cancer cell line.^gHuman breast cancer cell line.